Advanced neuroimaging in acute lymphoblastic leukemia and craniopharyngioma. Association with cognition and metabolism in adult childhood-onset survivors.

Svärd, Daniel

2021

Document Version:
Publisher's PDF, also known as Version of record

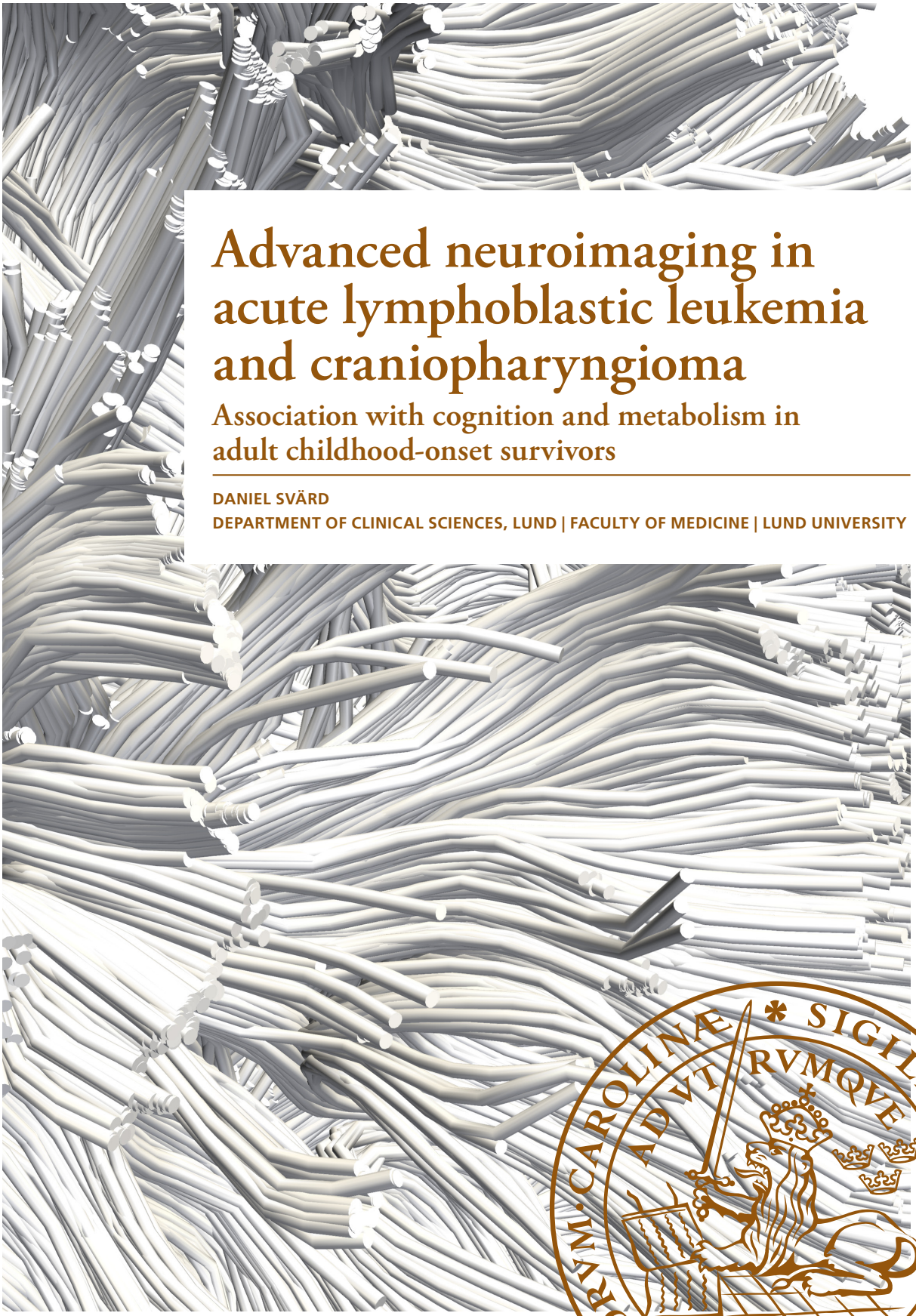

Advanced neuroimaging in acute lymphoblastic leukemia and craniopharyngioma

Association with cognition and metabolism in adult childhood-onset survivors

DANIEL SVÄRD
DEPARTMENT OF CLINICAL SCIENCES, LUND | FACULTY OF MEDICINE | LUND UNIVERSITY

Advanced neuroimaging in acute lymphoblastic leukemia and craniopharyngioma

Advanced neuroimaging in acute lymphoblastic leukemia and craniopharyngioma

Association with cognition and metabolism in adult childhood-onset survivors

Daniel Svärd

LUND
UNIVERSITY

DOCTORAL DISSERTATION

by due permission of the Faculty of Medicine, Lund University, Sweden.
To be defended at Segerfalksalen, BMC, Lund University
on the 26th of November 2021 at 08:00 (CET).

Faculty opponent
Professor Johan Wikström
Department of Surgical Sciences, Radiology, Uppsala University

Organization LUND UNIVERSITY	Document name DOCTORAL DISSERTATION
	Date of issue 2021-11-26
Author: Daniel Svärd	Sponsoring organization

Title and subtitle

Advanced neuroimaging in acute lymphoblastic leukemia and craniopharyngioma: association with cognition and metabolism in adult childhood-onset survivors

Abstract

Childhood-onset acute lymphoblastic leukemia (ALL) and craniopharyngioma (CP) are associated with cognitive impairment and metabolic complications mainly due to late complications after treatment and/or the neoplasia itself. Alterations in the brain and their association with cognitive and metabolic function in adult survivors have not been thoroughly studied. A better understanding of these alterations is a prerequisite for optimized treatment and follow-up care.

The main aim of this thesis was to study structural and functional alterations in the brain and their relation to cognition and metabolism in adult survivors of childhood-onset ALL, treated with chemotherapy and cranial radiotherapy (CRT), and in adults with childhood-onset CP, treated with surgery and in some cases additional CRT. Additionally, we first investigated potential confounders in the analyses to be able to interpret the results reliably.

In paper I, we investigated white matter hyperintensities as a confounder in statistical analysis of diffusion-weighted magnetic resonance imaging (MRI) and found that these may act as a confounder and therefore should be taken into consideration in the study design and when interpreting the results.

In paper II, we investigated microstructural alterations in the hypothalamus using diffusion tensor imaging (DTI) and found that alterations are seen in ALL but not in CP survivors without hypothalamic involvement of the tumor. These alterations were more pronounced in obese ALL survivors despite all subjects being on complete hormone substitution.

In paper III and IV, we investigated which cognitive domains that are affected in ALL and CP. Using DTI and diffusional kurtosis imaging, we also investigated microstructural alterations in the cingulum, the fornix, the uncinate fasciculus, and the hypothalamus. We found several cognitive domains affected and that alterations in the investigated structures correlated with deficits in different cognitive domains.

In paper V and VI, we investigated cognitive interference processing in ALL and CP, and its correlated neuronal activity using functional MRI. We found impaired cognitive interference processing in ALL but not in CP. We found no functional alterations in the cingulo-fronto-parietal attention network, or in any other part of the brain in neither patient group.

In conclusion, both childhood-onset ALL and CP survivors exhibit deficits in several cognitive domains and there is an association between these deficits and structural alterations in the investigated structures. The results are of importance for optimizing treatment and follow-up care. Further, they may also serve as models for a generalized diffuse brain injury and more focal brain injury, respectively, used to better understand similar conditions.

Key words: MRI, diffusion tensor imaging, diffusional kurtosis imaging, tractography, fMRI, acute lymphoblastic leukemia, craniopharyngioma

Classification system and/or index terms (if any):

Supplementary bibliographical information:		Language: English
ISSN: 1652-8220		ISBN: 978-91-8021-102-4
Recipient's notes:	Number of pages: 92	Price:
	Security classification:	

Signature  Date 2021-10-21

Advanced neuroimaging in acute lymphoblastic leukemia and craniopharyngioma

Association with cognition and metabolism in adult childhood-onset survivors

Daniel Svärd

LUND
UNIVERSITY

Cover photo by Daniel Svärd representing a visualization of a section of the white matter tracts of the author's brain

Faculty of Medicine
Department of Clinical Sciences, Lund

ISBN 978-91-8021-102-4
ISSN 1652-8220

Printed in Sweden by Media-Tryck, Lund University
Lund 2021

To my father

Table of Contents

Abstract

Childhood-onset acute lymphoblastic leukemia (ALL) and craniopharyngioma (CP) are associated with cognitive impairment and metabolic complications mainly due to late complications after treatment and/or the neoplasia itself. Alterations in the brain and their association with cognitive and metabolic function in adult survivors have not been thoroughly studied. A better understanding of these alterations is a prerequisite for optimized treatment and follow-up care.

The main aim of this thesis was to study structural and functional alterations in the brain and their relation to cognition and metabolism in adult survivors of childhood-onset ALL, treated with chemotherapy and cranial radiotherapy (CRT), and in adults with childhood-onset CP, treated with surgery and in some cases additional CRT. Additionally, we first investigated potential confounders in the analyses to be able to interpret the results reliably.

In paper I, we investigated white matter hyperintensities as a confounder in statistical analysis of diffusion-weighted magnetic resonance imaging (MRI) and found that these may act as a confounder and therefore should be taken into consideration in the study design and when interpreting the results.

In paper II, we investigated microstructural alterations in the hypothalamus using diffusion tensor imaging (DTI) and found that alterations are seen in ALL but not in CP survivors without hypothalamic involvement of the tumor. These alterations were more pronounced in obese ALL survivors despite all subjects being on complete hormone substitution.

In paper III and IV, we investigated which cognitive domains that are affected in ALL and CP. Using DTI and diffusional kurtosis imaging, we also investigated microstructural alterations in the cingulum, the fornix, the uncinate fasciculus, and the hypothalamus. We found several cognitive domains affected and that alterations in the investigated structures correlated with deficits in different cognitive domains.

In paper V and VI, we investigated cognitive interference processing in ALL and CP, and its correlated neuronal activity using functional MRI. We found impaired cognitive interference processing in ALL but not in CP. We found no functional alterations in the cingulo-fronto-parietal attention network, or in any other part of the brain in neither patient group.

In conclusion, both childhood-onset ALL and CP survivors exhibit deficits in several cognitive domains and there is an association between these deficits and structural alterations in the investigated structures. The results are of importance for optimizing treatment and follow-up care. Further, they may also serve as models for a generalized diffuse brain injury and more focal brain injury, respectively, used to better understand similar conditions.

List of original papers

This thesis is based upon the following papers, which are reproduced with the permission of the publishers, and referred to in the text by their Roman numerals:

I. Svärd D, Nilsson M, Lampinen B, Lätt J, Sundgren PC, Stomrud E, Minthon L, Hansson O, van Westen D. The effect of white matter hyperintensities on statistical analysis of diffusion tensor imaging in cognitively healthy elderly and prodromal Alzheimer's disease. *PLoS One.* 2017;12(9):e0185239.

II. Follin C, Fjalldal S, Svärd D, van Westen D, Gabery S, Petersén Å, Lätt J, Rylander L, Erfurth EM. Microstructure alterations in the hypothalamus in cranially radiated childhood leukemia survivors but not in craniopharyngioma patients unaffected by hypothalamic damage. *Clin Endocrinol (Oxf).* 2017;87(4):359-366.

III. Fjalldal S, Follin C, Svärd D, Rylander L, Gabery S, Petersén Å, van Westen D, Sundgren PC, Björkman-Burtscher IM, Lätt J, Ekman B, Johansson A, Erfurth EM. Microstructural white matter alterations and hippocampal volumes are associated with cognitive deficits in craniopharyngioma. *Eur J Endocrinol.* 2018;178(6):577-587.

IV. Follin C, Svärd D, van Westen D, Björkman-Burtscher IM, Sundgren PC, Fjalldal S, Lätt J, Nilsson M, Johanson A, Erfurth EM. Microstructural white matter alterations associated to neurocognitive deficits in childhood leukemia survivors treated with cranial radiotherapy - a diffusional kurtosis study. *Acta Oncol.* 2019;58(7):1021-8.

V. Svärd D, Follin C, Fjalldal S, Hellerstedt R, Mannfolk P, Mårtensson J, Sundgren P, Erfurth EM. Cognitive interference processing in adults with childhood craniopharyngioma using functional magnetic resonance imaging. *Endocrine.* 2021;10.1007/s12020-021-02824-9.

VI. Svärd D, Erfurth EM, Hellerstedt R, Mannfolk P, Mårtensson J, Sundgren P, Follin C. Cognitive interference processing in adult survivors of childhood acute lymphoblastic leukemia using functional magnetic resonance imaging. *Acta Oncol.* 2021;1-8.

Preface

This thesis is the summarized result of the collaboration between different research groups in various fields, such as neuroradiology, endocrinology, neuropsychology, neurology, and, last but not least, medical physics. With this thesis, I will try to present our combined efforts from a radiological point of view. The thesis comprises of six papers all in all.

Paper I is a methodological study, investigating potential confounders on diffusion-weighted MRI parameters. I designed the study, performed the analyses, interpreted the results, and wrote the manuscript. The study is based on data from the European Prospective Investigation into Diet and Cancer in the city of Malmö, Sweden, as well as from the Swedish BIOFINDER study, and was a collaboration between the Department of Diagnostic Radiology at Lund University, the Clinical Memory Research Unit at Lund University, and the MR Physics Group at Lund University. The conclusions in paper I are a prerequisite for the following papers.

Paper II-VI is based on data acquired between 2013-2014 in collaboration between the Department of Endocrinology and the Department of Oncology, both at Skåne University Hospital, Lund. In paper II-IV, I performed the MRI analyses. Further, I also took part in performing the statistical analyses, in the interpretation of the results, and in the writing of the manuscripts together with my co-authors. In paper V-VI, I performed the MRI analyses, the statistical analyses, the interpretation of the results, and I wrote the manuscripts. Paper II-VI was a collaboration between the Department of Diagnostic Radiology and the Department of Logopedics, Phoniatrics and Audiology, both at Lund University, and the Department of Endocrinology and the Department of Oncology, both at Skåne University Hospital. Paper III has previously been included in another doctoral thesis.

Abbreviations

AD	Axial diffusivity
ALL	Acute lymphoblastic leukemia
BMI	Body mass index
BOLD	Blood-oxygen-level-dependent
CFP	Cingulo-fronto-parietal
CNS	Central nervous system
CP	Craniopharyngioma
CRT	Cranial radiotherapy
CST	Corticospinal tract
dACC	Dorsal anterior cingulate cortex
DKI	Diffusional kurtosis imaging
DLPFC	Dorsolateral prefrontal cortex
dMRI	Diffusion-weighted magnetic resonance imaging
DTI	Diffusion tensor imaging
FA	Fractional anisotropy
fMRI	Functional magnetic resonance imaging
GH	Growth hormone
IGF-1	Insulin-like growth factor 1
MD	Mean diffusivity
MK	Mean kurtosis
MMSE	Mini mental state examination
MRI	Magnetic resonance imaging
MSIT	Multi-source interference task
NAWM	Normal-appearing white matter

RD	Radial diffusivity
RK	Radial kurtosis
ROI	Region of interest
SLF	Superior longitudinal fasciculus
TSH	Thyroid-stimulating hormone
WM	White matter
WMH	White matter hyperintensities

Background

Magnetic resonance imaging

Magnetic resonance imaging (MRI) is a technique that is based on the magnetic properties of the nuclei of certain atoms to generate image contrast. In a medical context, this is most commonly achieved using the hydrogen nuclei, due to their abundance in the human body. Under normal circumstances, it can be described as each hydrogen nucleus spinning around its own axis and by doing so creating a small magnetic moment. The magnetic moments are randomly oriented and, consequently, the net magnetization is zero. However, within a strong magnetic field, the magnetic moments tend to align along the axis of this field, which generates a net magnetization. Using an electromagnetic field with the same frequency as that of the hydrogen nucleus (i.e. the resonance frequency), it is possible to rotate the magnetic moment of the nucleus as long as the abovementioned electromagnetic field is applied. Thereafter, the nucleus will return to its equilibrium state and align along the main magnetic field. When this happens, the nucleus will generate a signal in the receiver coils via magnetic induction that can be recorded.

The MRI signal is dependent on what molecule the hydrogen nuclei is attached to, as well as on the molecular composition of the adjacent environment. By using different combinations of electromagnetic fields on the nuclei, different properties about the environment in which the nuclei dwells can be derived from the MRI signal. The process in which the nuclei return to their equilibrium state with their axis aligned to the main magnetic field is called *T1 relaxation* and depends on the interactions between the nucleus and its environment. *T2 relaxation* is dependent on the composition of adjacent molecules causing loss of coherence. Both the T1 and the T2 relaxation times differs between tissues, which is exploited to create unique imaging contrasts that can provide valuable information about the investigated tissue.

Diffusion-weighted MRI

Diffusion-weighted MRI (dMRI) uses magnetic field gradients to encode information on the random motion of water molecules, called diffusion, in different compartments of the human body. This is achieved by exposing a population of

water molecules to a magnetic gradient pulse, followed by an identical gradient with reversed polarity. In areas where water molecules diffuse more freely, a lot of water molecules will not be exposed to the exact same magnetic field changes and the MRI signal decreases, whereas in areas with more restricted diffusion, water molecules will be exposed to more of the same changes in the magnetic field and, therefore, the MRI signal will not decrease to the same extent. These properties can be used to probe for microstructural tissue alterations. For example, healthy neuronal tissue in the brain consists mostly of densely packed neurons, including dendrites and myelinated axons, that restrict diffusion of water molecules. If these structures were to degenerate, the diffusion would be less restricted and generate a different MRI signal compared to healthy tissue (Basser et al., 1994a; Le Bihan et al., 2001). There are several mathematical models that can be used to describe the amplitude and direction of diffusion of water molecules based on the MRI signal, some of which are described below.

Diffusion tensor imaging

When water molecules are contained in an environment without any obstacles, e.g. the cerebrospinal fluid, they diffuse freely and in no particular direction, i.e. the diffusion can be described as isotropic. In an environment consisting of grey matter, the diffusion is restricted by cell bodies, but the water molecules are still not more likely to diffuse in any particular direction, and hence the diffusion can still be roughly approximated as isotropic. However, in an environment consisting of white matter (WM), the myelinated axons will restrict the diffusion, and it will take shorter time for the water molecules to diffuse along the axons compared to perpendicular to them, due to less restriction in this direction, and therefore the diffusion can be described as anisotropic.

Diffusion tensor imaging (DTI) describes this type of anisotropic diffusion using a tensor, which is an algebraic object. The eigenvalues of the tensor, which are the factors by which the eigenvectors of the tensor is scaled, are commonly used to quantify the diffusion (Basser et al., 1994b; Pierpaoli et al., 1996; Johansen-Berg et al., 2009). To facilitate interpretation and comparison, four DTI parameters called mean diffusivity (MD), fractional anisotropy (FA), axial diffusivity (AD), and radial diffusivity (RD) are calculated from the eigenvalues. MD is the mean of the eigenvalues. FA is a quantification of anisotropy and ranges from 0-1, where 0 denotes isotropic diffusion and 1 denotes highest possible anisotropy. AD is the largest eigenvalue and hence describes the diffusivity along the principal direction of diffusion, whereas RD is the mean of the other two eigenvalues representing the diffusivity perpendicular to the principal direction of diffusion.

It has been proposed that the DTI parameters can be used to describe microstructural tissue integrity (Basser et al., 1994a; Pierpaoli et al., 1996; Le Bihan et al., 2003). For example, MD and RD are said to be associated with demyelination, whereas FA is associated with decreased WM integrity, and AD to be a marker for axonal loss

(Basser et al., 1994a; Alexander et al., 2007). However, even though the DTI parameters are associated with microstructural tissue integrity in some way, it is important to keep in mind that there are several known confounding effects that make interpretation of DTI parameters challenging under certain conditions. For example, partial degeneration of a WM tract in an area with crossing fiber bundles render a higher FA and can wrongfully be interpreted as increased microstructural integrity when the underlying process is actually the opposite (Douaud et al., 2010). Another possible pitfall is that the parameters cannot be used to differentiate between different microstructural histopathological changes (see the section below about potential confounders in the analysis of dMRI parameters).

Diffusional kurtosis imaging

Diffusional kurtosis imaging (DKI) is a theoretically more complex model compared to DTI and can be used to obtain more detailed information on the tissue microstructure (Nørhøj, 2018). Kurtosis is a statistical measure that can be used to approximate how non-Gaussian the diffusion is. This means that DKI could be more useful in complex tissue composition, because the degree of non-Gaussian diffusivity increases with increasing tissue complexity. Different parameters can be calculated from the DKI model; the mean kurtosis (MK) describes the mean diffusion kurtosis across all directions, and the radial kurtosis (RK) is the diffusion kurtosis perpendicular to the direction of the principal diffusion direction (Nørhøj, 2018).

Tractography

dMRI can also be used for tracking WM tracts of the brain. The simplified theoretical background is as follows: it can be assumed that the principal direction of diffusion in one voxel, which can be described as a three-dimensional pixel, is also the principal direction of the myelinated axons in the same voxel. Thus, if one follows the principal direction of diffusion in a deterministic way, from voxel to voxel, one should be able to delineate the underlying WM tracts. This technique is called deterministic tractography and can be used to segment WM tracts for investigation of connectivity between different regions of the brain (Mori and Barker, 1999; Basser et al., 2000). The segmented tracts can also be assessed in terms of microstructural integrity using extracted DTI/DKI parameters from selected parts of the tracts. However, even though more advanced models have developed during recent years, e.g. probabilistic methods and so-called constrained spherical deconvolution (Tournier et al., 2007), they are still a simplification of the underlaying composition of the WM and should be used with awareness of their limitations. For example, the deterministic model based on the FA is not particularly reliable when it comes to tracking fibers in regions with e.g. crossing fibers. Also, when it comes to segmenting WM tracts, this can be done in several different ways, from manual segmentation in subject-space to fully automated atlas-based methods,

meaning that comparisons between studies are somewhat challenging to interpret if the procedures are not carefully described.

Potential confounders in statistical analysis of dMRI

WM hyperintensities (WMH), also known as WM lesions, WM changes, or leukoaraiosis, are defined as areas in the WM with high T2-signal in otherwise normal-appearing WM (NAWM) and are thought to represent chronic ischemia due to small vessel disease (Fazekas et al., 1987; Potter et al., 2010; Gouw et al., 2011; Schmidt et al., 2011; Wardlaw et al., 2013). These alterations are commonly asymptomatic, and the prevalence increases with age (Breteler et al., 1994; Ylikoski et al., 1995; Longstreth et al., 1996; de Leeuw et al., 2001). DTI is sensitive to WMH and there is an association between elevated MD and reduced FA in affected WM regions (Jones et al., 1999; Vernooij et al., 2008; Maillard et al., 2011; Leritz et al., 2014; Maillard et al., 2014; de Groot et al., 2015; Pelletier et al., 2016). Because of this, unequal WMH load between two groups may potentially confound group comparisons, leading to differences being partially due to the difference in WMH load rather than differences in more disease-specific alterations in NAWM. However, this methodological issue is not always considered and accounted for in DTI research, and the magnitude of the effect of WMH on DTI parameters has not yet been fully investigated.

Functional MRI

MRI can be used to investigate neuronal activity in response to e.g. performing a specific task. Blood-oxygen-level-dependent (BOLD) imaging is based upon the assumption that neurons increase their metabolism and thus their oxygen and carbohydrate consumption when activated (Ogawa et al., 1990; Ogawa et al., 1992). When there is an increased need for oxygen and metabolites in the tissue, blood vessels react with temporary vasodilation so that the blood volume can temporarily increase to meet the increased demand. Oxygenated and deoxygenated hemoglobin have different magnetic properties; deoxygenated hemoglobin causes inhomogeneities in the magnetic field affecting mainly T2-relaxation. Hence, the MRI signal will decrease in areas with more oxygenated hemoglobin, which is the physical background to the BOLD imaging contrast. The technique is, however, not quantitative, which means that interpretation of only one measurement of the signal will not be meaningful. To make meaningful interpretations, the signal must be sampled multiple times during the performance of different tasks. In the simplest task-based fMRI experiment, the signal is measured during a baseline control task, compared to another task, and the response function is fitted to the data. In principle, the difference in signal will be interpreted as the neuronal activity required to perform the non-baseline task. This information can be used to visualize which

functional networks are activated when performing different tasks and to compare activation on a group level.

Structural networks

The WM of the brain constitutes the structural network between neurons and can be anatomically segmented into different WM tracts as described below. Association fiber tracts connect cortical regions in the ipsilateral hemisphere, and include the cingulum, the uncinate fasciculus, the superior longitudinal fasciculus, the inferior longitudinal fasciculus, and the inferior fronto-occipital fasciculus. They are important for higher cortical functions, such as memory, emotions, language, visuospatial abilities, and praxis. Commissural fiber tracts connect cortical regions in the contralateral hemisphere, and include the corpus callosum, the anterior commissure, and the hippocampal commissure of the fornix. They are important for integration of cognition, perception, and motor function. Projection fiber tracts connect cortical regions to subcortical structures, and include the corticospinal tract, the corticobulbar tract, the thalamic radiation, as well as the main part of the fornix. They are important for motor function, perception, and cognition.

Cingulum

The cingulum is an association fiber tract that is considered part of the limbic system, see Figure 2 and 4, and is important for attention, memory function, and emotions (Bush et al., 2000; Lin et al., 2014; Koenig et al., 2015; Özyurt et al., 2017). It consists of long-running fibers as well as short U-fibers that connect the cingulate cortex with the frontal, parietal, occipital, and temporal lobes. The longest fibers originate in the amygdala, the uncus, and the parahippocampal gyrus, and run in the medial temporal lobe, the occipital lobe, and the cingulate gyrus before terminating in the frontal lobe. The shorter U-fibers connect adjacent areas of the medial frontal gyrus, the precuneus, the cingulate, lingual, and fusiform gyri. Because of suggested different anatomical properties, the cingulum can be further subdivided into a dorsal component which constitutes most of the WM in the cingulate gyrus, and a ventral component running within the parahippocampal gyrus, the retrosplenial cingulate gyrus, and the posterior precuneus (Park et al., 2004; Gong et al., 2005; Wakana et al., 2007).

Fornix

The fornix is mainly a projection fiber tract, see Figure 4, and is considered part of the limbic system. Fibers originate in the hippocampus and terminate in the mamillary bodies, the anterior thalamus, and in the hypothalamus; it also has a minor commissural component consisting of the hippocampal commissure (Insel

and Takehara-Nishiuchi, 2013; Jin and Maren, 2015). The fornix is important for memory function (Zhuang et al., 2013; Douet and Chang, 2015).

Uncinate fasciculus

The uncinate fasciculus is an association fiber tract, see Figure 4, that is considered part of the limbic system, and is important for episodic and semantic memory, emotions, and language (Olson et al., 2015; Daianu et al., 2016). In humans, it is one of the last major WM tracts to mature and this process is not finished until the early fourth decade of life (Lebel et al., 2012). The uncinate fasciculus connects the anterior temporal lobe with the orbitofrontal cortex (Klingler and Gloor, 1960).

Superior longitudinal fasciculus

The superior longitudinal fasciculus (SLF) is an association fiber tract, see Figure 2, consisting of long-running fibers as well as short U-fibers, connecting the perisylvian cortex of the frontal, parietal, and temporal lobes. The left SLF is considered important for language, verbal working memory, and praxis, while the right SLF is considered important for visuospatial processing as well as some aspects of language, such as prosody and semantics (Cannestra et al., 2000; Castillo et al., 2001; Sabsevitz et al., 2005; Jardri et al., 2007; Martin-Loeches et al., 2008).

Corticospinal tract

The corticospinal tract (CST) is a projection fiber tract, see Figure 2, that originate in the frontal cortex and run through the posterior limb of the corona radiate, the internal capsule, and the cerebral peduncles, further through the so-called pyramids in the medulla oblongata, where most fibers cross the midline to the contralateral side, before forming the lateral column in the spinal cord; it is important mainly for voluntarily motor function (Behrens et al., 2003; Newton et al., 2006)

Functional networks

Functional networks, or large-scale brain networks, can be defined as different spatially remote brain regions exhibiting temporal association in activity, that is functional connectivity, as visualized using e.g. fMRI. Due to variations in the algorithms and parameters used to identify these networks, the number and compositions of identified networks vary, and there is also more or less overlap between the different networks. The most commonly recognized networks are briefly discussed below.

Medial fronto-parietal default mode network

The medial fronto-parietal default mode network consists anatomically of the medial prefrontal cortex, the posterior cingulate cortex/precuneus, and the angular gyrus. It is active when the brain is at wakeful rest and the individual is not focused on external stimuli (Raichle, 2015). It is also involved in internally-oriented tasks such as daydreaming and mind-wandering as well as envisioning the future, retrieving memories, and theory of mind (Raichle, 2015).

Midcingulo-insular salience network

The midcingulo-insular salience network primarily consists of the anterior insula and the dACC. It is important for monitoring and filtering the salience of external stimuli and internal cognitive input as well as recruiting relevant functional networks (Menon and Uddin, 2010). It contributes to a wide variety of higher functions, including communication, social behavior, and self-awareness through the integration of sensory, emotional, and cognitive information (Menon and Uddin, 2010).

Lateral fronto-parietal central executive network

The lateral fronto-parietal central executive network consists anatomically of the DLPFC and the posterior parietal cortex (Uddin et al., 2019). It is important for sustained attention, complex problem-solving, and working memory (Menon, 2011).

Cingulo-fronto-parietal attention network

The cingulo-fronto-parietal (CFP) attention network is partially overlapping with the salience network as well as the central executive network and consists mainly of the dACC and the DLPFC. It is important for target detection, novelty detection, error detection, decision-making, response selection, and stimulus/response competition, and cognitive interference processing, which is the ability to be attentive to goal-relevant information and at the same to be able to reject goal-irrelevant information (Bush et al., 2003; Bush et al., 2006).

Hypothalamus

The hypothalamus is considered part of the limbic system and contains several small nuclei with a variety of functions (Schneeberger et al., 2014). It forms the ventral part of the diencephalon and is situated below the thalamus. Anteriorly, it borders with the anterior commissure and the optic chiasm, posteriorly with the posterior commissure and the mamillary bodies, laterally and superiorly with the thalamus. The hypothalamus exerts many of its functions thorough acting as a link between

the central nervous system (CNS) and the endocrine system via the pituitary gland. It is responsible for several homeostatic functions, e.g. the regulation of blood flow and energy metabolism, as well as the regulation of reproductive activity, and coordination of responses to threatening conditions (Schneeberger et al., 2014). To be able to monitor and modulate these diverse functions, it receives sensory and contextual information, which is compared to biological set points, and relevant visceral motor, neuroendocrine, and/or somatic motor effector systems are activated to restore homeostasis and/or elicit appropriate behavioral responses.

Induction of a hypothalamic lesion can result from breaching the floor of the third ventricle, distortion or pulling causing shear stress to the vessels of the median eminence, or radiation to the area (de Vile et al., 1996). If a lesion occurs, the abovementioned functions can be disturbed.

Studies using DTI to investigate microstructural integrity in the hypothalamus in humans a scarce (Alkan et al., 2007; Menzler et al., 2012). In otherwise healthy, obese subjects, microstructural alterations in the hypothalamus were associated with a decline in cognitive performance (Puig et al., 2015). In children with CP, the consequences of a hypothalamic lesion have been investigated with fMRI showing altered fMRI activity in the medial prefrontal cortex during memory retrieval (Özyurt et al., 2017). Thus, a hypothalamic lesion may also indirectly lead to frontal and medial temporal lobe dysfunction, causing deficits in memory, attention, and executive function (Özyurt et al., 2014b).

Acute lymphoblastic leukemia

Acute lymphoblastic leukemia (ALL) constitutes the largest group of childhood cancer. With an annual incidence of 35-40 cases per 1 million children it accounts for approximately one out of four cases of all childhood malignancies (Howlader et al., 2020). The disease has a peak incidence at around 4 years of age and is slightly more common in boys than in girls (Plasschaert et al. 2004).

The patients present with an increased number of immature blood cells and a reduced number of normal blood cells. Signs and symptoms include fatigue, pallor, petechiae, bleeding, fever, weight loss, bone pain, and dyspnea. In case of leukemic spread, lymphadenopathy and hepatosplenomegaly may be present. During later stages of the disease, the CNS may also be involved, presenting with headache, nausea and vomiting, lethargy, irritability, nuchal rigidity, and papillary edema. The testes may also be affected with leukemic infiltration, presenting as painless testicular enlargement.

ALL treatment regimens include a remission-induction phase, a consolidation phase, and continuation therapy to eliminate residual disease. Chemotherapy in

combination with cranial radiotherapy (CRT) were standard treatment in Sweden between 1971-1992. Today, CRT is only used for treating a minority of high risk ALL and in reduced doses because of the now well-known association between this type of treatment and common late complications after treatment such as cognitive impairment, anterior-pituitary deficiencies, growth retardation, obesity, cardiovascular mortality, osteoporosis/osteopenia, and meningiomas (Sklar et al., 2000; Lustig et al., 2003; Link et al., 2004; Follin et al., 2006; Schuitema et el., 2015; Chemaitilly et al., 2018). Intermediate and low risk ALL are given intensified systemic and intrathecal chemotherapy instead of CRT.

Because of the increased survival rate in pediatric patients, the prevalence of late complications after treatment has also increased. The exact mechanism of radiation-induced damage to the CNS is not known, but direct damage to the cell nucleus as well as a vascular etiology has been proposed. Certain areas of the CNS seem to be more sensitive to radiation-induced damage than others, and animal studies have shown that the hypothalamus is particularly vulnerable (Arnold, 1954; Rahmathulla et al., 2013). Pituitary hormone deficiencies are commonly seen in radiated ALL survivors, and it has been suggested that the damage may be related to hypothalamic damage (Larkins and Martin, 1973; Littley et al., 1989; Sathiavageeswaran et al., 2007). Interestingly, there is a clear difference in the incidence in pituitary hormone deficiencies, with growth hormone (GH) being the most frequently affected, followed by gonadotropin, adrenocorticotrophic hormone, and thyroid-stimulating hormone (TSH), suggesting different radiosensitivity to the hypothalamic-pituitary axis (Littley et al., 1989). Despite hormone substitution, metabolic complications are seen, particularly in female ALL survivors, suggesting a possible hypothalamic dysfunction (Follin et al., 2016).

Cognitive impairment in ALL survivors include deficits in attention, short-term memory, working memory, inhibition, cognitive flexibility, learning, fine motor coordination, and visuospatial abilities (Ochs et al., 1991; Link et al., 2006; Schuitema et al., 2015). Cognitive outcomes for patients treated with CRT and chemotherapy are worse compared to treatment with chemotherapy alone (Halsey et al., 2011; Cheung and Krull, 2015). Further, diagnosis and treatment at a younger age seem to be associated with more adverse cognitive outcomes most likely because the immature brain is more sensitive to treatment related neurotoxic effects, and because these effects also may interfere with the ongoing maturation of the brain (Edelstein et al., 2011; Halsey et al., 2011). Additionally, some studies have reported that female ALL survivors are at somewhat greater risk of cognitive impairment compared to males (Kirchhoff et al., 2011; Schuitema et al., 2015). It is of great importance to fully disentangle the nature of the cognitive impairment seen in ALL survivors, since it has a large impact on these individuals' ability of independent living (Mody et al., 2008; Kirchhoff et al., 2011; Kunin-Batson et al., 2011).

A limited number of studies have used DTI in adult childhood-onset ALL survivors and reported alterations in FA in WM tracts in the frontal, parietal, and temporal

lobes, and that these alterations were associated with cognitive impairment, such as deficits in sustained attention, visuomotor control, and visuospatial sequencing (Schuitema et al., 2013). No previous studies have investigated structural alterations in ALL with DKI. Additionally, the relationship between structural alterations and related cognitive and metabolic symptoms have not yet been thoroughly studied.

Five previous studies have used task-based fMRI to investigate functional alterations in relation to cognitive function in ALL survivors (Robinson et al., 2010; Armstrong et al., 2013; Monje et al., 2013; Krull et al., 2016; Fellah et al., 2019). Increased fMRI activity in the dorsal anterior cingulate cortex (dACC) and the dorsolateral prefrontal cortex (DLPFC) has been reported during the visual N-back task to assess working memory (Robinson et al., 2010). Another study reported increased fMRI activity in the hippocampus during an auditory cued recall memory task (Armstrong et al., 2013). A third study reported increased fMRI activity in several areas, including the claustrum, during a paradigm used to test episodic visual memory (Monje et al., 2013). A positive correlation between intravenous methotrexate concentration during treatment and fMRI activity in the frontal and anterior cingulate cortices, the caudate nuclei, and the putamen has also been reported during the attention network test (Krull et al., 2016). Another study reported a correlation between diagnosis at a younger age, as well as higher intravenous methotrexate concentration during treatment, and decreased fMRI activity in the parietal and temporal lobes during the continuous performance task and the attention network task to assess sustained attention, alerting, orienting, and conflict (Fellah et al., 2019).

Craniopharyngioma

Craniopharyngioma (CP) is a rare, benign pituitary tumor with an aggressive growth pattern and high morbidity and mortality, primarily due to the hypothalamic involvement of the disease (Bülow et al, 1998; Tomlinson et al., 2001; Müller et al., 2004; Pereira et al., 2005; Holmer et al., 2009; Holmer et al., 2010; Müller, 2011; Müller et al., 2011b; Olsson et al., 2015). The tumor is thought to arise from Rathke's pouch, which is an embryological structure that gives rise to the adenohypophysis. The incidence of the disease is 1.3-1.7 per million inhabitants per year, without any significant difference in gender distribution; approximately one-third of all cases occur during childhood (Bunin et al., 1998; Olsson et al., 2015).

Histopathologically, CP can be subdivided into a adamantinomatous, a papillary, and a mixed-type form, where the first-mentioned is most commonly seen in childhood (Erfurth et al., 2013; Müller, 2013). The signs and symptoms in childhood-onset CP include headaches, visual field defects, hypothalamic

dysfunction, and failure to thrive (Müller et al., 2004; Erfurth et al., 2013; Müller, 2013).

Due to the frequent hypothalamic involvement, CP is regarded as a complicated disease with a wide range of co-morbidities that include cognitive impairment due to neuroendocrine dysfunction, and metabolic complications including morbid obesity and increased cardiovascular mortality (Bülow et al., 1998; Pereira et al., 2005; Holmer et al., 2009; Müller et al., 2011; Özyurt et al., 2014a; Olsson et al., 2015; Özyurt et al., 2015). Adult survivors of childhood-onset CP, especially patients with hypothalamic involvement, are at risk of cognitive impairment, with deficits in memory, attention, and processing speed, even on complete hormone replacement therapy (Fjalldal et al., 2013; Özyurt et al., 2014b). However, individuals where the hypothalamus is unaffected by the tumor has a more favorable risk profile (Müller et al., 2004; Holmer et al., 2009; Müller et al., 2011). Therefore, a paradigm shift in treatment regimens has recently been seen, from total surgical removal of the tumor to a more individualized and conservative approach of subtotal removal (Merchant et al., 2002; Schubert et al., 2009; Müller, 2017).

It is plausible that the focal hypothalamic lesion induces distal changes in hypothalamic networks through the processes of diaschisis and/or transneuronal degeneration, which may also contribute to the cognitive impairment in these individuals (Müller, 2019). Different neuroimaging techniques, including dMRI and fMRI, have recently been used to investigate the association between cognitive impairment and metabolic complications in CP survivors, to explain the underlaying mechanisms behind these deficits (Roth et al., 2012; Özyurt et al., 2014b; Özyurt et al., 2017). These studies reported decreased fMRI activity during the premeal test and increased fMRI activity during the post-meal test as compared to controls (Roth et al., 2012), and differential recruitment of fronto-limbic brain regions during emotional face recognition (Özyurt et al., 2014b). However, the relationship between structural and functional alterations and their related cognitive and metabolic symptoms have not yet been thoroughly studied in these patients.

Rationale

Adult childhood-onset ALL survivors as well as CP survivors have cognitive deficits and metabolic complications to a varying degree. It is reasonable to suspect that this is due to a combination of both the neoplasia itself and its concomitant treatment. In ALL survivors, the primary damage to the brain can, due to the localization of the disease and its subsequent treatment, be suspected to be more general, whereas in CP survivors, the damage ought to, once again due to the localization of the disease and its subsequent treatment, be more focal, and primarily located in the area of the pituitary gland and the hypothalamus.

In both conditions, the primary lesions may induce further neurodegeneration of nearby as well as remotely connected structures and thus accentuate the neurodegenerative process. Given the nature of the diseases, the current available treatment, and the complex symptomatology that ALL and CP survivors exhibit, it is reasonable to suspect that alterations in the hypothalamus and its associated structural and functional networks are at least partially responsible for the cognitive deficits and metabolic complications associated with these conditions.

Previous studies have used advanced neuroimaging to some extent. However, alterations in structural and functional networks and their association to cognitive and metabolic function in areas of the brain that can be suspected to be affected by these conditions have not been fully investigated. Understanding the pathophysiology and extent of these alterations is crucial for characterizing these conditions, and to be able to optimize treatment and follow-up support for the individuals.

Aims

The overall aim of this thesis was to investigate structural and functional alterations in the brain and their relation to cognitive deficits and metabolic complications in adult survivors of childhood-onset ALL, treated with CRT and chemotherapy, and in adults with childhood-onset CP, treated with surgery and in some cases with additional CRT. Specific aims were as follows:

1. To study WMH as a confounder in statistical analysis of DTI parameters (Paper I), which was a prerequisite for the following aims.
2. To study microstructural alterations in the WM tracts of the dorsal and ventral cingulum, the fornix, the uncinate fasciculus, and in the hypothalamus using dMRI (more specifically DTI and DKI), and to relate these to cognitive and metabolic function (Paper II-IV).
3. To study functional alterations in neuronal activity during cognitive interference processing using fMRI, and to relate these to behavioral performance (Paper V-VI).

Subjects

Paper I

Cognitively healthy elderly

Cognitively healthy elderly (n = 132; mean (SD) age 71.6 (4.5) years; 44.7% males) were recruited from the Malmö Diet and Cancer study, an epidemiological study that is part of the European Prospective Investigation into Diet and Cancer in the city of Malmö, Sweden and the Swedish BIOFINDER study (Manjer et al., 2001; Janelidze et al., 2016). Inclusion criteria were age > 60 years, scoring 27−30 points on Mini Mental State Examination (MMSE) at screening visit (Folstein et al., 1975), non-pathological Amyloid-β 42/40 ratio (i.e. Amyloid-β 42/40 > 0.1), no subjective cognitive impairment, and fluency in the Swedish language. Exclusion criteria were presence of severe neurological disease (e.g. stroke, Parkinson's disease or multiple sclerosis) or psychiatric disease (e.g. severe depression or psychotic syndromes) (Gustavsson et al., 2015).

Two subgroups with unequal WMH load, matched for age, gender, prevalence of cardiovascular disease, MMSE score, and ventricle volume, were selected from the group of cognitively healthy elderly (Figure 1). Lower WMH load was defined as having a WMH volume ≤ 0.5% of the total intracranial volume, which corresponded approximately to Fazekas grade 0–1, and higher WMH load as having a WMH volume ≥ 1%, which corresponded approximately to Fazekas grade 2–3 (Fazekas et al., 1987).

Prodromal Alzheimer's disease subjects

Subjects with amnestic mild cognitive impairment (n = 83; mean (SD) age 71.4 (5.4) years; 53.0% males) and pathological Amyloid-β 42/40 ratio (i.e. Amyloid-β 42/40 ≤ 0.1), indicating high risk of conversion to Alzheimer's disease, were selected from the Swedish BIOFINDER study (Janelidze et al., 2016). Inclusion criteria were subjective cognitive impairment, objective memory impairment according to neuropsychological assessments, not fulfilling criteria for dementia, scoring 24−30 points on MMSE, age 60−80 years, and fluency in the Swedish language. Exclusion

criteria were cognitive impairment that without doubt could be explained by another condition (other than prodromal dementia) and severe somatic disease.

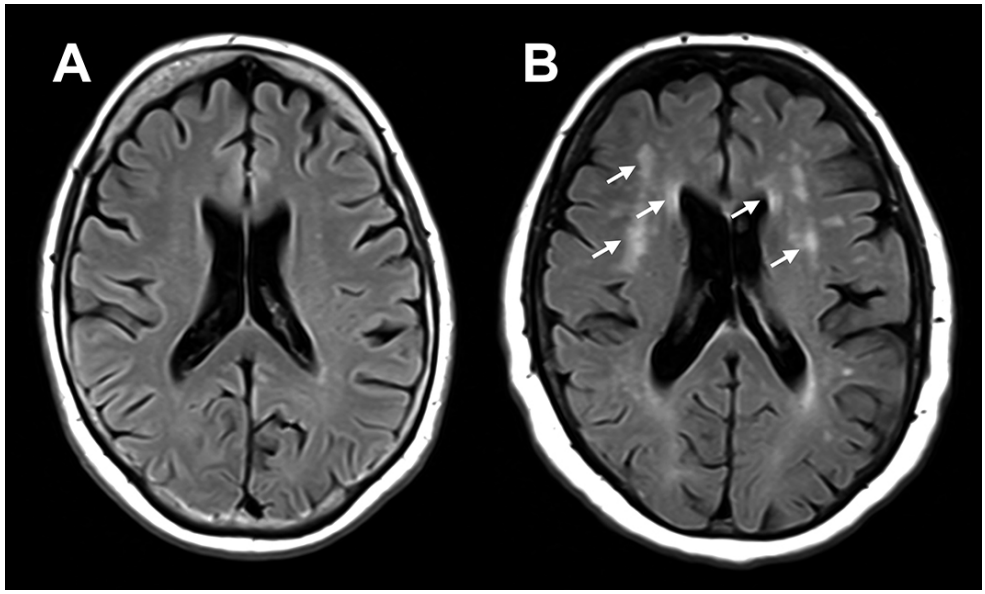

Figure 1.
Transverse FLAIR images of two different representative subjects from paper I with different white matter hyperintensity (WMH) load. Subject A represents the subgroup with lower WMH load (i.e. a WMH volume ≤ 0.5% of the intracranial volume, which corresponded approximately to Fazekas grade 0–1) and subject B represents the subgroup with higher WMH load (i.e. a WMH volume ≥ 1% of the intracranial volume, which corresponded approximately to Fazekas grade 2–3); arrows indicate examples of regions with WMH.

Paper II-VI

Adult childhood-onset acute lymphoblastic leukemia survivors

Fifty-eight patients from the Southern Region of Sweden (population 2.5 million) were treated for childhood-onset ALL with chemotherapy and CRT (24 Gy) at Lund University Hospital in Sweden between 1971 and 1992. ALL survivors treated with CRT (18 Gy) and chemotherapy, or chemotherapy only were not included. Eight subjects out of the 58 subjects were not tested for pituitary hormone function due to declined participation, illness or breastfeeding, and 12 subjects declined participation, mainly due to lack of time. Therefore, 38 ALL survivors (21 females) were included in the study. All subjects had received CRT (24 Gy) and chemotherapy (intrathecal and intravenous) according to the common protocols of the Nordic countries at that time (Gustafsson et al., 1981). Median (range) age at

investigation 38 (27–46) years and median (range) time from CRT was 34 (23–42) years.

All subjects were on complete hormone substitution for median (range) 11 (3–13) years, including substitution with GH (median [range] 0.4 mg/day 0.2–0.8) due to GH deficiency in childhood (n = 3) or adulthood (n = 35). Further, 16 subjects were on thyroxine, 1 was on hydrocortisone due to adrenal insufficiency, 3 females were supplemented with estrogens due to primary amenorrhea, 8 females used contraceptives, and 6 males were substituted with testosterone due to radiotherapy to the testes. One male had diabetes mellitus type 2. None were smokers.

In paper II, all 38 subjects were included in the analysis of metabolic function, while 29 subjects were included in the MRI investigation of the hypothalamus, since 9 were excluded due to difficulties performing the MRI acquisition or data not fulfilling certain criteria (see below).

In paper IV, 38 subjects were included in the neuropsychological assessment and 31 subjects were investigated with MRI, since 7 were excluded due to difficulties performing the MRI acquisition or data not fulfilling certain criteria (see below).

In paper VI, 26 subjects were included in the fMRI analysis, since 10 subjects had difficulties performing the MRI acquisition or data not fulfilling certain criteria (see below) and another two subjects were excluded because they did not understand how to perform the fMRI task.

Adult childhood-onset craniopharyngioma survivors

Sixty-four patients from the Southern Region of Sweden (population 2.5 million), who were treated for childhood-onset CP at Lund University Hospital between 1958 and 2010, were invited to participate in the study. Forty-one (24 females) subjects with a median (range) age at investigation of 35 (17–56) years in women, and 36 (20–49) years in men, were included. Excluded subjects (n = 23) were either assessed to be too ill (meningioma n = 1, neuromuscular disease n = 1, living in a home for disabled n = 2), too busy (n = 6), investigations too stressful according to patients (n = 2), had aneurysm clip (n = 1), did not give any reason (n = 7), had missing medical records (n = 1), or did not reply (n = 2).

Included subjects were treated with surgical removal of the tumor. In addition, 16 subjects had also received CRT directed towards the area of the tumor (median [range] dose 50 [35–55] Gy). Age at first operation was median (range) 12 (3–29) years in women and median (range) 9 (3–22) years in men. Time since first operation was median (range) 21 (6–49) years in women and median (range) 23 (11– 42) years in men.

All subjects were supplemented with GH (median [range] 0.6 [0.4–1.2] mg/day for females and median [range] 0.5 [0.2–0.8] mg/day for men) resulting in

normalization of insulin-like growth factor 1 (IGF-1). Eighty-three percent of the females and 88% of the males received thyroxine. Five subjects had normal adrenocorticotropic-cortisol axes and all others needed hydrocortisone. Seventy-one percent of the females were substituted with estrogens due to primary amenorrhea and one female also had androgen supplementation. Eighty-two percent of the males were substituted with testosterone. Twenty-five subjects had normal visual acuity (≥ 0.5) along with normal or minor visual field defects. None of the subjects were smokers.

The tumor location was graded retrospectively by an experienced neurosurgeon, based on each subjects' medical records as: intra-sellar growth, supra-sellar growth, or supra-sellar growth toward or into the third ventricle. The latter was the criterion for hypothalamic involvement, which was found in 23 subjects (Fjalldal et al., 2019).

In paper II, 17 subjects without hypothalamic involvement were included. One subject was excluded due to incomplete MRI examination.

In paper III, all the 41 subjects were included in the neuropsychological assessment, while 5 subjects had to be excluded from the MRI examination due to the presence of either a shunt causing significant artifacts (n = 1), pacemaker (n = 1), claustrophobia (n = 2), or weight restrictions (n = 1). Four subjects had to be excluded from the DTI analysis due to unsuccessful post-processing. Additionally, one more subject involved in the analysis of only the fornix and the hypothalamus was excluded as data did not fulfill quality criteria for region of interest (ROI) definition. Further, six subjects were excluded from the DTI analyses of the hypothalamus, as the extent of hypothalamic involvement prevented the data to fulfill the quality criteria for ROI definition. This resulted in a total of 32 patients completing the DTI part of the MRI analysis except for the analysis of the fornix (n = 31) and the hypothalamus (n = 25).

In paper V, one subject was excluded due to difficulties in understanding how to perform the fMRI task, one subject was excluded due to excessive motion during fMRI acquisition, and six subjects were excluded due to partially missing data. Thus, 28 CP survivors were included in paper V.

Control subjects

A total of 31 control subjects were recruited from a pool of 10 potential subjects per ALL/CP survivor, matched for age, gender, and smoking habits, that were selected randomly from a computerized register of the population in the catchment area of the patients (Link et al., 2006). Twenty of these subjects had participated in a previous study (Fjalldal et al., 2013). Twelve new subjects were recruited using the same method (Link et al., 2006). One subject did not complete MRI examination due to claustrophobia and another was excluded from the DTI analysis involving

the hypothalamus in paper II and III, based on quality criteria. Thus, of these 31 subjects, data from 27 subjects (media [range] age 38 [27–46] years; 12 females) were used in paper II, 31 subjects (18 females) in paper III, 29 subjects (16 females) in paper IV, 29 subjects (median [interquartile range] age 37.0 [32.5–42.0] years; 17 females) in paper V, and 26 subjects (median [interquartile range] age 37.5 [33.0–41.5] years; 15 females) in paper VI. The slightly different composition of the control group during the different analyses in paper II-VI ensured that the control group was matched to the ALL and CP survivors, respectively, regarding age, gender, and smoking habits in the different comparisons.

Ethical considerations

All subjects gave written informed consent. The studies of paper I-VI were approved by the local ethics committee (DNR 2011/769, 2011/770, and 2012/596).

Methods

Diffusion-weighted MRI

Paper I

MRI acquisition

dMRI data were acquired on a Siemens Trio 3 T MRI scanner equipped with a standard 12-channel head coil using a single-shot EPI sequence (TR/TE 8200/86 ms/ms) with diffusion encoding in 64 directions and *b* values of 0 and 1000 s/mm. In total, 60 contiguous transverse slices with a spatial resolution of 2×2×2 mm^3 were acquired.

For the assessment of WMH, 27 transverse slices of T2-weighted FLAIR imaging were acquired (TR/TE/TI 9000/89/2500 ms/ms/ms) at a spatial resolution of 0.7×0.7×5.2 mm^3 as well as a coronal T1-weighted MP-RAGE sequence (TR/TE/TI 1950/3.37/900 ms/ms/ms), with a spatial resolution of 1.0×1.0×1.2 mm^3 and a flip angle of 9˚.

Post-processing

DTI data were corrected for motion and eddy current induced artifacts using Elastix (Klein et al., 2010). DTI volumes of MD and FA were calculated from the diffusion tensor eigenvalues using in-house developed software implemented in Matlab (MATLAB 2013a, The MathWorks Inc., Natick, MA, USA). DTI volumes were registered to MNI152 standard-space using the registration algorithm of FLIRT and FNIRT, parts of the FMRIB Software Library (Jenkinson et al., 2011). Subjects that exhibited excessive motion artifacts or incidental findings such as meningioma, severe atrophy or old infarction were excluded.

Segmentation y of white matter tracts

Tractography of the dorsal and ventral cingulum, the SLF, and the CST was performed using a semi-automated method, which utilized multiple ROIs defined in MNI152 standard-space and warped to subject-space (Figure 2). In subject-space, the ROIs were used as Boolean operators to segment streamlines from a deterministic whole-brain tractography generated in TrackVis; thresholds were set

to 0.2 for FA and 30˚ for the angle. This method was shown to be more reliable and robust, less biased by inter- and intra-individual anatomical variation, less dependent on correct position of the head in the MRI scanner, and less time-consuming compared to manual definition of ROIs in subject-space (Nucifora et al., 2012).

ROIs in standard space were defined as follows. To include streamlines running along the whole WM tract an 'AND' ROI covering the entire WM tract was defined for each of the four tracts, according to the ICBM-DTI-81 WM labels atlas (Mori et al., 2005). To exclude intersecting streamlines from adjacent WM tracts, a 'NOT' ROI was defined around the anatomical region of the segmented tract according to the JHU WM tractography atlas (Hua et al., 2008). The procedure was performed using in-house developed software implemented in Matlab, utilizing the warp-fields generated by FNIRT to warp ROIs from standard-space to subject-space, and TrackVis for streamline management. All segmented WM tracts were visually inspected, and, if necessary, adjusted in subject-space.

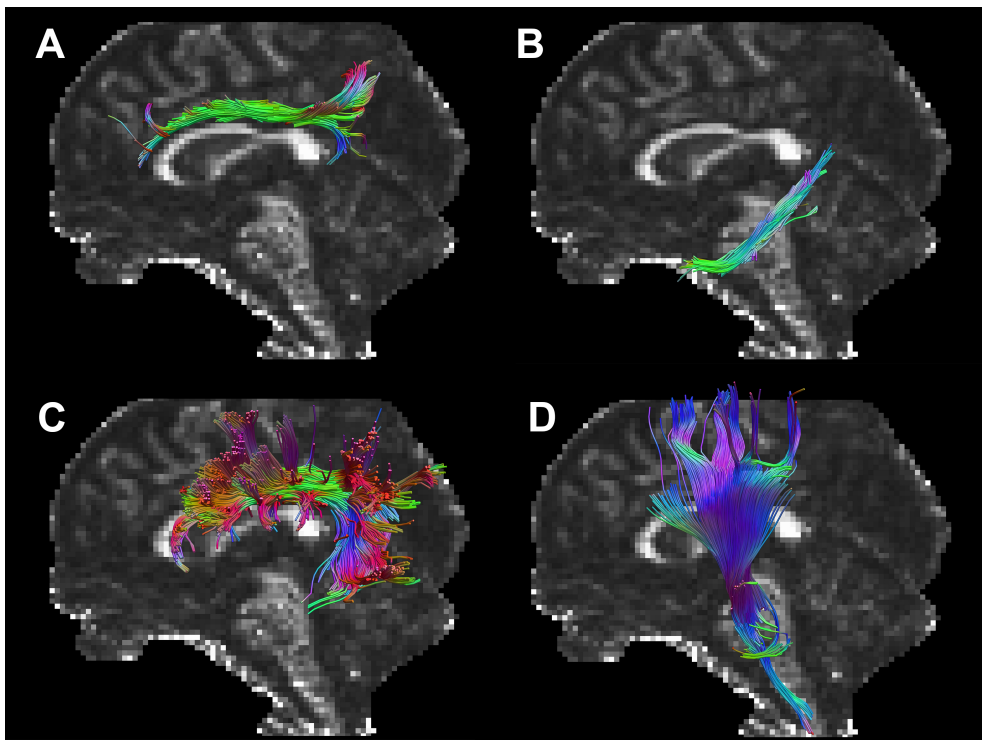

Figure 2.
Color-coded (red = right-left; green = anterior-posterior; blue = cranial-caudal) visualization of the segmented white matter tracts analyzed in paper I, superimposed on a mid-sagittal fractional anisotropy map, in a representative subject: the dorsal cingulum (A), the ventral cingulum (B), the superior longitudinal fasciculus (C), and the corticospinal tract (D).

Assessment of WMH load

Automated segmentation of WMH volume (ml) was performed using Lesion segmentation tool (LST as implemented in SPM8) on T2-weighted FLAIR imaging and T1-weighted MP-RAGE volumes. Additionally, WMH load was also graded by an experienced neuroradiologist using the Fazekas scale (Fazekas et al., 1987).

Paper II-IV

MRI acquisition

dMRI data were acquired on a 3 T MRI scanner (MAGNETOM Skyra, Siemens Healthcare, Erlangen, Germany) equipped with a 20-channel head/neck receiver coil. DTI data consisted of three volumes acquired with $b = 0$ s/mm^2, followed by 32 volumes acquired using b values of 250, 500, and 1000 s/mm^2, distributed over 6, 6, and 20 directions, respectively. Fifty-two contiguous transverse slices were acquired using a single-shot EPI (TR/TE 8100/103 ms/ms) sequence with a spatial resolution of 2.3×2.3×2.3 mm^3. DKI data consisted of three volumes acquired with $b = 0$ s/mm^2, followed by 96 volumes acquired using b values of 250, 500, 1000, and 2750 s/mm^2 distributed over 6, 6, 20, and 64 directions, respectively. Fifty-two contiguous transverse slices were acquired using a single-shot EPI (TR/TE 8100/103 ms/ms) sequence with a spatial resolution of 2.3×2.3×2.3 mm^3.

Additionally, transverse T1-weighted MP-RAGE volumes were acquired (1 mm isotropic resolution, TR/TE 1900/3 ms/ms, flip angle 9°) and used in the analysis of the hypothalamus as described below.

Post-processing

To correct for eddy current and motion artifacts, volume registration using ElastiX with interpolated references was performed (Klein et al., 2010). DTI volumes (FA, MD, AD, and RD) and DKI volumes (MK and RK) were calculated using in-house developed software, implemented in Matlab (MATLAB 2013a, The MathWorks Inc., Natick, MA). Here, the diffusion and kurtosis tensors were fitted by non-linear optimization as in Lätt et al. (2013). The fitting only allowed positive values of the diffusion tensor eigenvalues. In a small number of voxels where the kurtosis was below zero, the fitting was repeated after additional smoothing was performed. DTI and DKI volumes were registered to MNI152 standard space and to the T1-weighted MP-RAGE volumes using the registration algorithm of FLIRT and FNIRT (part of the FMRIB Software Library), and ElastiX, respectively (Klein et al., 2010; Jenkinson et al., 2011). The resolution of the resulting parameter maps was 1×1×1mm^3.

Delineation of the hypothalamus

A multi-slice ROI was manually defined on coronal subject-space T1-weighted MP-RAGE volumes in the right and the left hypothalamus according to Gabery et al. (2015). Briefly, the most anterior section was set where the optic chiasm attaches to the ventral part of the septal area at bregma level 1.3 mm. A superior border was drawn as a straight line from the hypothalamic sulcus to the most lateral point of the optic tract throughout the region. The inferior border was set at the junction to the optical chiasm for anterior sections, and once the chiasm was no longer visible in more posterior sections, the border was set at the level of the infundibular nucleus and defined by the border to cerebrospinal fluid. The final posterior border was set at the level when the fornix appeared and merged with the mamillary nucleus at bregma level 9.3 mm. The optical tract was excluded from all measurements. These ROIs were used to calculate the DTI parameters from the co-registered DTI volumes and used in the statistical analyses described below (Figure 3).

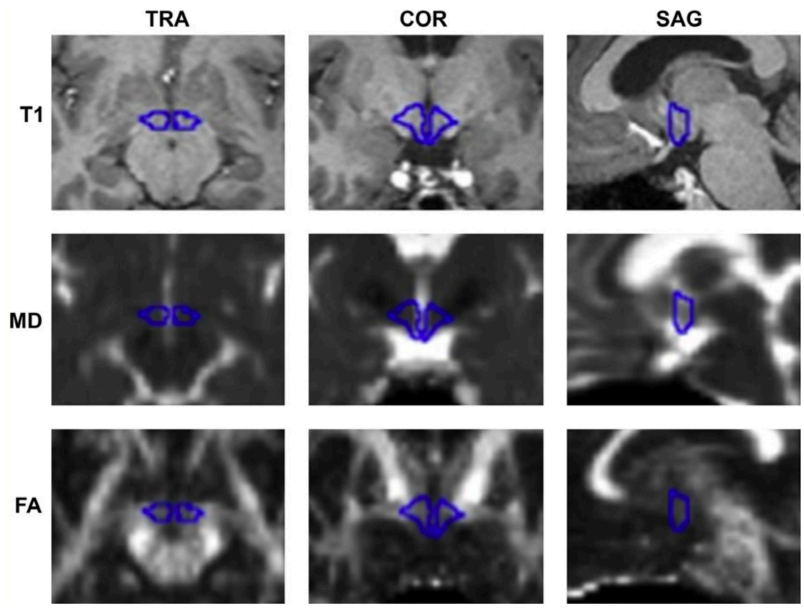

Figure 3.
Multi-slice region of interest defined on T1-weighted MP-RAGE volume, visualized on a transverse (TRA), coronal (COR), and sagittal (SAG) plane, respectively, and used to calculate the diffusion tensor imaging parameters mean diffusivity (MD) and fractional anisotrophy (FA) of the hypothalamus.

Segmentation of white matter tracts

Tractography was performed using deterministic tracking based on constrained spherical deconvolution (implemented in MRtrix version 0.2, $L_{max} = 8$, using the $b = 2750$ s/mm^2 shell only) to extract mean parameters from the dorsal and ventral cingulum, the fornix, and the uncinate fasciculus, see Figure 3 (Lätt et al., 2013).

All tracts were generated using one seed ROI covering the entire tract in multiple slices. Multiple ROIs were used to segment the different tracts based on Boolean operations. All ROIs were defined in MNI152 standard-space and warped back to subject-space utilizing the warp-fields generated by FNIRT.

The dorsal cingulum was defined using two ‘AND’ ROIs around the tract, superior to the genu and splenium, respectively, and one ‘NOT’ ROI across one mid-sagittal slice. The ventral cingulum was defined using two ‘AND’ ROIs around the tract, rostral to the pons and inferior to the splenium, respectively, and one ‘NOT’ ROI across one mid-sagittal slice (Figure 4). The fornix was defined using two ‘AND’ ROIs around the body of the fornix, caudal to the anterior pillars, and around the crus fornici, inferior to the splenium, respectively, and three ‘NOT’ ROIs, rostral to the anterior pillars, caudal to the crus fornici, and through the corpus callosum on in the transverse plane, respectively (Figure 4). The uncinate fasciculus was defined using two ‘AND’ ROIs around the tract, rostral to the genu, and around the tract where it bends into the temporal lobe ventral to the upper pons, respectively, and three ‘NOT’ ROIs caudal to the front of the pons, through the corpus callosum in the transverse plane, and across one mid-sagittal slice, respectively (Figure 4).

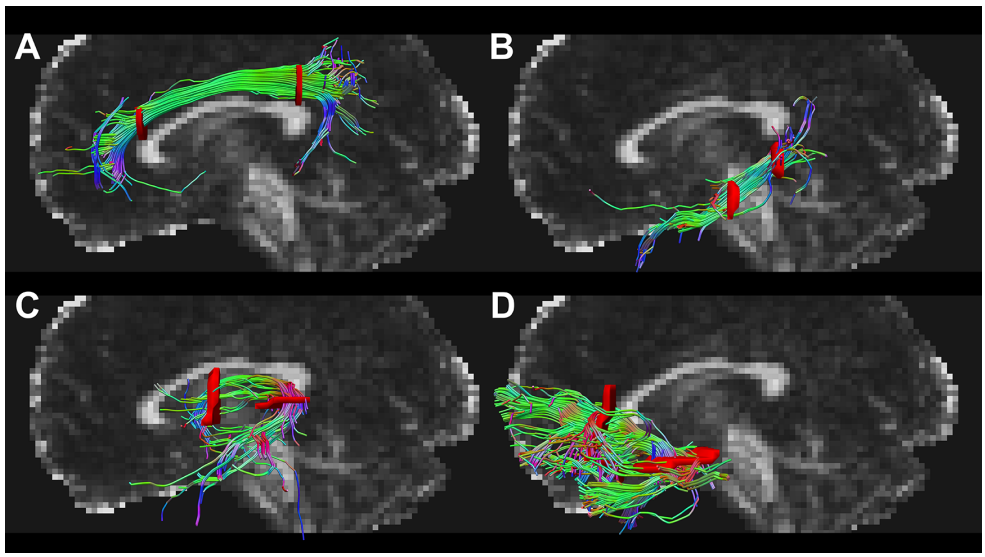

Figure 4.
Color-coded (red = right-left; green = anterior-posterior; blue = cranial-caudal) visualization of the segmented white matter tracts analyzed in paper III and IV, superimposed on a mid-sagittal fractional anisotropy map in a representative subject: the dorsal cingulum (A), the ventral cingulum (B), the fornix (C), and the uncinate fasciculus (D). Red region of interests (ROIs) indicating the position of Boolean 'AND' ROIs warped from MNI152 standard-space to subject space and used to segment the white matter tracts from a deterministic whole-brain tractography.

If the total number of streamlines generated for each WM tract were < 100, the ROIs utilized for definition of the specific WM tract were visually inspected and adjusted

if not located in the intended anatomical region. The mean DTI/DKI parameters for each WM tract were used in the statistical analyses described below.

Functional MRI

Paper V-VI

MRI acquisition

fMRI data were acquired on the same 3T MRI scanner used to acquired dMRI data in Paper II-IV. A gradient-echo EPI sequence (TR/TE 1500/30 ms/ms, 25 slices, 64 dynamic scans, voxel size = 3×3×4 mm^3) was used to acquire data. To perform the fMRI analyses described below, an additional T1-weighted MP-RAGE sequence (TR/TE 1900/2.54 ms/ms), with 1 mm^3 isotropic resolution, was also acquired.

Post-processing

fMRI data were processed and analyzed using FEAT from FMRIB's Software Library (www.fmrib.ox.ac.uk/fsl). Registration to standard-space was carried out using linear registration (FLIRT) followed by non-linear registration (FNIRT) (Jenkinson et al., 2001; Jenkinson et al., 2002). The following pre-statistics processing was applied: motion correction using MCFLIRT (Jenkinson et al., 2002); slice-timing correction using Fourier-space time-series phase-shifting; non-brain removal using BET (Smith, 2002); spatial smoothing using a Gaussian kernel of FWHM 5mm; grand-mean intensity normalization of the entire 4D dataset by a single multiplicative factor; high-pass temporal filtering (Gaussian-weighted least-squares straight line fitting, with sigma = 45.0 s).

fMRI task

Cognitive interference processing, which is the ability to be attentive to goal-relevant information, and at the same time to be able to reject goal-irrelevant information, can be tested using the multi-source interference task (MSIT). MSIT has been shown to reliably activate the CFP attention network, and includes the dACC and the DLPFC, which are important for target detection, novelty detection, error detection, decision-making, response selection, and stimulus/response competition (Bush et al., 2003; Bush et al., 2006). The MSIT was performed according to Bush et al. (2006). Briefly, the subjects were given an MRI-compatible three-button keypad and told that the keypad buttons represented the numbers 1, 2, and 3, from left to right. The subjects were then instructed to use the right index, middle, and ring finger to respond. All subjects were right-handed and had or were corrected to normal vision. They were also informed that three numbers would appear in the center of the screen every few seconds. The objective was to report,

via button-press, the identity of the displayed number that differed from the other two distractor numbers (Figure 5). During the control tasks, the distractors were zeros, and the target numbers (either 1, 2, or 3) were always placed congruently with their position. During the interference tasks, the distractors were either 1, 2, or 3, and the target numbers (either 1, 2, or 3) were never placed congruently with their position. After receiving instructions, each subject performed the MSIT once, to make sure that they could perform the task correctly. Next, each subject performed the MSIT during fMRI data acquisition.

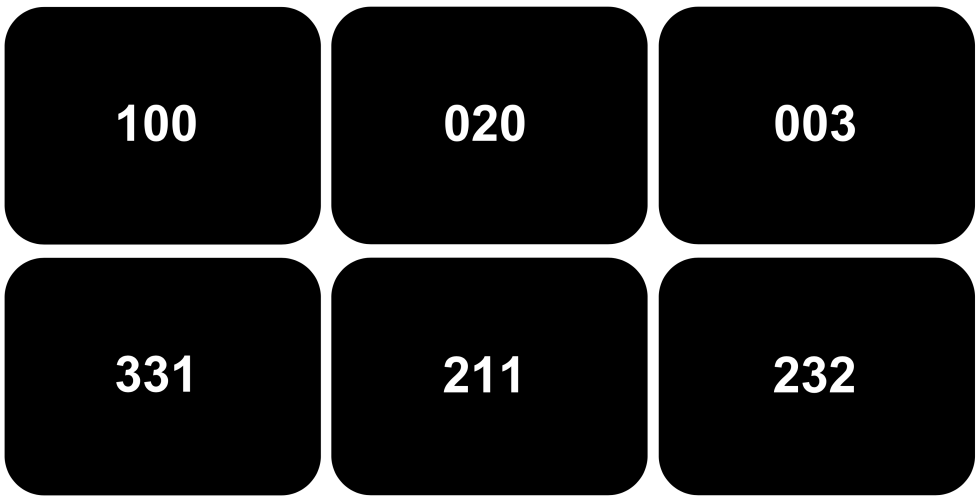

Figure 5.
The multi-source interference task tests cognitive interference processing, which is the ability to be attentive to goal-relevant information, and at the same time to be able to reject goal-irrelevant information. During the test, the objective was to report the identity of the displayed number that differed from the other two numbers; during the control tasks (upper row), the distractors were zeros, and the target numbers (either 1, 2, or 3) were always placed congruently with their position. During the interference tasks (lower row), the distractors were either 1, 2, or 3, and the target numbers were never placed congruently with their position. The correct answer for the first column is hence '1', for the second '2', and for the third '3'.

The subjects completed two scans each with a few minutes long break between the scans. Each scan was 396 sec long, including a 30 sec fixation dot at the start and at the end. Between the fixation dots, four 42 sec long blocks of the control tasks alternated with four 42 sec of the interference tasks without any interruption between blocks. Each block consisted of 24 three digit-number combinations, meaning that the subjects had 1.75 sec to solve each task. Response times (ms), accuracy performance (%), and missing responses were recorded using E-prime 2.0 (Psychology Software Tools, Pittsburgh, PA).

Neuropsychological assessment

Paper III-IV

Neuropsychological assessment was administered by two psychologists using a fixed battery order consisting of the following cognitive tests:

- Wechsler Adult Intelligence Scale Vocabulary (testing semantic memory)
- Rey Auditory Verbal Learning Test for immediate recall (1-2 min), delayed recall (30 min), and recognition (testing episodic verbal memory)
- Rey Complex Figure Test for immediate recall (1-2 min), delayed recall (30 min), and recognition (testing episodic visual memory)
- Wechsler Adult Intelligence Scale Digit Span (testing working memory)
- Wechsler Adult Intelligence Scale Digit Span Backward Subtest and Symbol-Coding (testing executive function, attention, and processing speed)
- Trail Making Test (testing executive function, attention, and processing speed)
- Rey Complex Figure Test Copy Subtest (testing visuospatial abilities)
- Wechsler Adult Intelligence Scale Block Design (testing visuospatial abilities)
- APT k-test (testing sustained attention)

It is common to convert the raw score to a 'standard score', which facilitates comparisons with previous studies. However, the raw score is more suitable when investigating a correlation to another variable and also in comparison with matched control subjects. Therefore, the raw score was used in the statistical analyses described below.

Anthropometric and biochemical assessment

Paper II-VI

The following anthropometric and biochemical measurements were used to characterize the study populations in paper II-VI and used as proxy variables for metabolic function in the analyses in paper II. Anthropometric measurements

included body height and weight, and was used to calculated body mass index (BMI) (kg/m^2). Biochemical analyses included glucose, insulin, leptin, IGF-1, TSH, free triiodothyronine, free thyroxine, cortisol, oestradiol, and testosterone. All blood samples were drawn in the morning after an over-night fast.

Statistical analysis

Paper I

A parametric two-tailed Student's *t*-test for independent samples was performed to compare MD and FA in the dorsal and ventral cingulum, the SLF, and the CST between the two matched subgroups of cognitively healthy elderly with different WMH load. A parametric test was chosen because of the relatively large group sizes and because MD and FA were approximately normally distributed. The effect size was based on differences in group means and described in a standardized manner using Cohen's *d*, which is defined as the difference between two means divided by a standard deviation for the data, that facilitates comparison between studies.

Two multivariate linear regression models were used to test if and to what degree the WMH load affected DTI parameters in prodromal Alzheimer's disease. In model 1, the dependent variable was MD or FA for each WM tract, while the independent variables were having prodromal Alzheimer's disease or not. In model 2, WMH volume was added as an additional independent variable. Standardized β was calculated to describe the effect of the independent variables. R^2 was calculated to describe the proportion of the variance in the dependent variable that was predictable from the independent variable (i.e. how well the regression model explained the real data). ΔR^2 was calculated to describe how R^2 changes between model 1 and 2 (i.e. if adjusting the analysis for WMH volume improved the explanatory power of the analysis).

P-value < 0.05 was regarded as statistically significant. Statistical analysis was performed using the Statistical Package for Social Sciences (SPSS version 22, IBM Corp., Chicago, IL, USA).

Paper II-IV

Non-parametric statistics were consistently used due to relatively small group sizes and for some of the parameters relatively skewed distributions. Differences between groups were compared using the Mann-Whitney *U* test. Among the CP survivors, bivariate correlations were assessed using Pearson correlation coefficient. To ensure that the assumption of linearity was reasonable, scatter plots were investigated.

Bivariate correlations among ALL survivors were assessed using Spearman's rank correlation coefficient. *P*-value < 0.05 was regarded as statistically significant. Bonferroni correction for multiple comparisons was performed for the 12 tests covering learning capacity and memory and the nine tests covering executive functions and attention, respectively, in ALL survivors. Statistical analyses were performed using the Statistical Package for Social Sciences (SPSS version 21 and 22, IBM Corp., Chicago, IL, USA).

Paper V-VI

Due to relatively small group sizes, parameters could not be assumed to be normally distributed and therefore non-parametric tests were used. Comparisons between groups were performed using the Mann-Whitney *U* test. The Wilcoxon signed-rank test was used to compare differences in response time and accuracy performance between interference and control tasks within the groups. Calculations were made using Statistical Package for Social Sciences (SPSS version 26, IBM Corp., Chicago, IL, USA). Results were regarded as statistically significant if $p < 0.05$.

An exploratory whole-brain fMRI analysis approach was used. fMRI contrasts of the interference effect for lower-level analyses were generated through the subtraction of fMRI signal during the control tasks from the interference tasks for each subject. The contrasts from the lower-level analysis for each subject were used to make group contrasts in an additional higher-level analysis to compare the group mean interference effect between the ALL survivors and the controls. Time-series statistical analysis was carried out using FILM with local autocorrelation correction (Woolrich et al., 2001). Z statistic images were thresholded non-parametrically using clusters determined by $Z > 3.1$ and a (corrected) cluster significance threshold of $p < 0.05$. The general linear model for both lower and higher level analyses was created using FLAME (FMRIB's Local Analysis of Mixed Effects) stage 1 (Beckmann et al., 2003; Woolrich et al., 2004; Woolrich, 2008).

Results

Paper I

In cognitively healthy elderly with higher WMH load, compared to lower WMH load, MD was increased in the right and left SLF, and in the right dorsal cingulum, and FA was reduced in the right and left SLF, and in the left dorsal cingulum (Table 1). The effect size, described as Cohen's *d*, ranged from small (ventral cingulum, $d < 0.3$) to very high (SLF, $d > 1.0$).

Table 1.
Comparison of mean diffusivity and fractional anisotropy in the investigated white matter tracts between the matched subgroups of cognitively healthy elderly with lower[a] and higher[b] WMH load, respectively. Values denote DTI parameters MD and FA in the respective tract (mean±SD). Effect size is expressed as Cohen's *d*.

	MD (μm²/ms)			FA		
	Cognitively healthy elderly with lower[a] WMH load (*n* = 21)	Cognitively healthy elderly with higher[b] WMH load (*n* = 21)	Cohen's *d*	Cognitively healthy elderly with lower[a] WMH load (*n* = 21)	Cognitively healthy elderly with higher[b] WMH load (*n* = 21)	Cohen's *d*
DC right	0.74±0.03	0.76±0.04	0.63*	0.44±0.02	0.43±0.03	−0.52
DC left	0.74±0.04	0.77±0.04	0.61	0.47±0.03	0.45±0.03	−0.69*
VC right	0.71±0.05	0.71±0.07	0.05	0.39±0.02	0.39±0.02	−0.09
VC left	0.70±0.05	0.72±0.06	0.37	0.39±0.02	0.38±0.03	−0.42
SLF right	0.75±0.03	0.81±0.06	1.24*	0.43±0.02	0.41±0.03	−1.04*
SLF left	0.73±0.03	0.79±0.06	1.27*	0.44±0.02	0.41±0.03	−1.06*
CST right	0.69±0.05	0.71±0.06	0.39	0.53±0.03	0.52±0.03	−0.34
CST left	0.69±0.04	0.71±0.06	0.38	0.53±0.03	0.53±0.04	0.01

[a]WMH volume ≤ 0.5% of the intracranial volume, which corresponded approximately to Fazekas grade 0–1.

[b]WMH volume ≥ 1% of the intracranial volume, which corresponded approximately to Fazekas grade 2–3.

CST = corticospinal tract; DC = dorsal cingulum; FA = fractional anisotropy; MD = mean diffusivity; SLF = superior longitudinal fasciculus; VC = ventral cingulum; WMH = white matter hyperintensities.

Standardized β for having prodromal Alzheimer's disease (independent variable) was significant for both MD and FA in the right and left SLF, and in the right and left dorsal and ventral cingulum (Table 2). R^2 ranged from 0.02 to 0.09. When WMH volume was added as an additional independent variable, standardized β for having prodromal Alzheimer's disease was significant for both MD and FA in the right and left ventral cingulum, and for FA in the right and left dorsal cingulum as well. Standardized β for WMH volume was significant for both MD and FA in the right

and left SLF, in the right and left dorsal cingulum, and in the right and left CST. ΔR^2 was significant in all analyses where standardized β for WMH volume was significant and ranged from 0.02 to 0.46.

Table 2.

Multivariate linear regression analyses of mean diffusivity (MD) and fractional anisotropy (FA) in the dorsal and ventral cingulum, the superior longitudinal fasciculus, and the corticospinal tract in cognitively healthy elderly and prodromal Alzheimer's disease subjects, unadjusted (model 1) and adjusted (model 2) for WMH volume, respectively. In model 1, the dependent variable was MD or FA for each investigated white matter tract and the independent variable were having prodromal Alzheimer's disease or not. In model 2, WMH volume was added as an additional independent variable. Only standardized β for having prodromal Alzheimer's disease and WMH volume are reported here.

		Model 1 (unadjusted for WMH)		Model 2 (adjusted for WMH)		
		Standardized β (Prodromal AD)	R^2	Standardized β (Prodromal AD)	Standardized β (WMH-volume)	ΔR^2
MD	DC right	0.16*	0.03	0.12	0.21*	0.04*
	DC left	0.15*	0.02	0.09	0.26*	0.06*
	VC right	0.23*	0.05	0.23*	n.s.	n.s.
	VC left	0.27*	0.07	0.24*	n.s.	n.s.
	SLF right	0.19*	0.07	n.s.	0.74*	0.46*
	SLF left	0.20*	0.06	n.s.	0.74*	0.46*
	CST right	n.s.	0.02	n.s.	0.29*	0.07*
	CST left	n.s.	0.01	n.s.	0.24*	0.05*
FA	DC right	−0.23*	0.09	−0.16*	−0.28*	0.07*
	DC left	−0.20*	0.06	−0.16*	−0.17*	0.02*
	VC right	−0.18*	0.04	−0.18*	n.s.	n.s.
	VC left	−0.24*	0.06	−0.21*	n.s.	n.s.
	SLF right	−0.13*	0.03	n.s.	−0.61*	0.32*
	SLF left	−0.16*	0.04	n.s.	−0.61*	0.32*
	CST right	n.s.	0.04	n.s.	−0.33*	0.09*
	CST left	n.s.	0.09	n.s.	−0.21*	0.04*

AD = Alzheimer's disease; CST = corticospinal tract; DC = dorsal cingulum; FA = fractional anisotropy; MD = mean diffusivity; SLF = superior longitudinal fasciculus; VC = ventral cingulum; WMH = white matter hyperintensities.

* denotes $p < 0.05$

n.s. denotes non-significant.

Paper II

ALL survivors had higher BMI, glucose, and insulin compared to controls. There were no differences in IGF-1, TSH, thyroxine, cortisol, or testosterone between ALL survivors and controls.

In ALL survivors, MD, AD, and RD was increased in the right and left hypothalamus, and FA was reduced in the right hypothalamus, compared to controls (Table 3). There were no differences in DTI parameters in the hypothalamus between the subgroup of CP survivors without hypothalamic involvement and controls.

Table 3.
Comparison of diffusion tensor imaging parameters fractional anisotropy, mean diffusivity, axial diffusivity, and radial diffusivity in the hypothalamus between ALL survivors and controls, and between CP survivors without hypothalamic involvement and controls.

	ALL survivors (n=29) Median (range)	CP survivors (n=17) Median (range)	Controls (n=27) Median (range)	ALL vs Controls *P*-values	CP vs Controls *P*-values
Right HT					
FA	0.27 (0.20-0.34)	0.29 (0.19-0.35)	0.29 (0.25-0.35)	.04	NS
MD	1.13 (0.89-1.24)	0.97 (0.85-1.10)	1.00 (0.77-1.21)	<.001	NS
AD	1.41 (1.18-1.64)	1.21 (1.11-1.37)	1.25 (1.02-1.49)	<.001	NS
RD	0.99 (0.74-1.19)	0.85(0.72-0.99)	0.86 (0.65-1.07)	<.001	NS
Left HT					
FA	0.30 (0.20-0.35)	0.32 (0.22-0.36)	0.31 (0.25-0.34)	NS	NS
MD	1.00 (0.76-1.08)	0.87 (0.72-1.01)	0.93 (0.78-1.12)	.01	NS
AD	1.27 (0.97-1.37)	1.14 (0.97-1.31)	1.18 (1.01-1.39)	.01	NS
RD	0.87 (0.66-0.97)	0.73 (0.60-0.89)	0.79 (0.65-0.98)	.01	NS

AD = axial diffusivity; ALL = acute lymphoblastic leukemia; CP = craniopharyngioma; FA = fractional anisotropy; HT = hypothalamus; MD = mean diffusivity; NS = non-significant; RD = radial diffusivity.

In ALL survivors with BMI ≥ 25, MD and AD was increased in the right hypothalamus compared to ALL survivors with BMI < 25. There were no differences in DTI parameters in the hypothalamus in CP survivors without hypothalamic involvement and with BMI ≥ 25 compared to BMI < 25 or in controls with BMI ≥ 25 compared to < 25.

No correlations were found between DTI parameters in the hypothalamus and BMI, fat mass, plasma glucose, insulin or leptin levels in ALL survivors or among CP survivors without hypothalamic involvement.

Paper III

There were no differences in any of the cognitive tests between CP survivors and controls. The subgroup of CP survivors with hypothalamic involvement scored lower than controls on Wechsler Adult Intelligence Scale Vocabulary (testing semantic memory), Rey Auditory Verbal Learning Test (testing episodic verbal memory), Rey Complex Figure Test (testing episodic visual memory), and Trail Making Test (testing executive function, attention, and processing speed).

In CP survivors and the subgroup of CP survivors with hypothalamic involvement, MD was increased, and FA reduced in the right uncinate fasciculus compared to controls. There were no differences in DTI parameters in the cingulum, in the fornix, or in the hypothalamus compared to controls.

In the right dorsal cingulum, MD correlated negatively with scoring on Rey Complex Figure Test (testing episodic visual memory) and Wechsler Adult Intelligence Scale Digit Span Backward Subtest (testing executive function,

attention, and processing speed) among CP survivors. In the right dorsal cingulum, FA correlated positively with scoring on Rey Complex Figure Test (testing episodic visual memory) and Wechsler Adult Intelligence Scale Block Design (testing visuospatial abilities) among CP survivors. In the right and left ventral cingulum, MD correlated negatively with scoring on Rey Complex Figure Test (testing episodic visual memory) among CP survivors (Figure 6). In the right uncinate fasciculus, FA correlated positively with scoring on Wechsler Adult Intelligence Scale Vocabulary (testing semantic memory) among CP survivors.

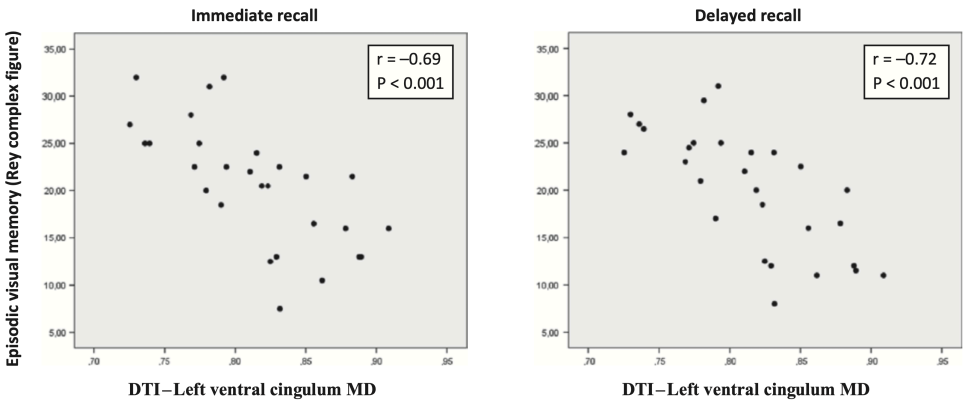

Figure 6.
Visualization of correlation between diffusion tensor imaging (DTI) parameter mean diffusivity (MD) in the left ventral cingulum and scoring on Rey Complex Figure Test (testing episodic visual memory) during immediate recall and delayed recall among 32 adult childhood-onset craniopharyngioma survivors (r = Pearson correlation coefficient).

No significant correlations between DTI parameters and scoring on cognitive test were found among controls.

Paper IV

The ALL survivors scored lower on all cognitive tests, i.e. Wechsler Adult Intelligence Scale Vocabulary (testing semantic memory), Rey Auditory Verbal Learning Test (testing episodic verbal memory), Rey Complex Figure Test (testing episodic visual memory test), Wechsler Adult Intelligence Scale Digit Span (testing working memory), Wechsler Adult Intelligence Scale Digit Span Backward Subtest (testing executive function, attention, and processing speed), Wechsler Adult Intelligence Scale Digit Symbol-Coding (testing executive function, attention, and processing speed), Trail Making Test (testing executive function, attention, and processing speed), Rey Complex Figure Test Copy Subtest (testing visuospatial abilities), Wechsler Adult Intelligence Scale Block Design (testing visuospatial abilities), and APT k-test (testing sustained attention), compared to controls.

In ALL survivors, MD was increased in the left uncinate fasciculus, FA was reduced in the right and left ventral cingulum, in the fornix, and in the right and left uncinate fasciculus, and RD was increased in the left ventral cingulum, and in the right and left uncinate fasciculus compared to controls. Further, MK was reduced in the right and left dorsal and ventral cingulum, and in the right uncinate fasciculus, and RK was reduced in the right and left dorsal and ventral cingulum, the fornix, and the right and left uncinate fasciculus.

In the right ventral cingulum, FA correlated positively, and MD, AD, RD correlated negatively with scoring on Rey Complex Figure Test (testing episodic visual memory) among ALL survivors. In the fornix, FA correlated positively, and MD, AD, RD correlated negatively with scoring on Rey Auditory Verbal Learning Test (testing episodic verbal memory) among ALL survivors. In the right uncinate fasciculus, FA correlated positively, and MD and RD correlated negatively with scoring on Rey Complex Figure Test (testing episodic visual memory) among ALL survivors (Figure 7).

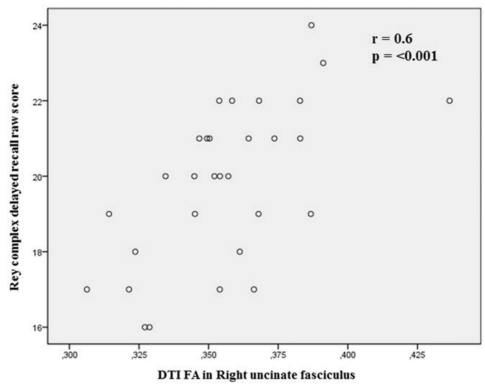

Figure 7.
Visualization of correlation between diffusion tensor imaging (DTI) parameter fractional anisotropy (FA) in the right uncinate fasciculus and scoring on Rey Complex Figure Test (testing episodic visual memory) during delayed recall among 31 adult childhood-onset acute lymphoblastic leukemia survivors (r = Spearman's rank correlation coefficient).

In the right ventral cingulum, MK correlated positively with scoring on Rey Complex Figure Test (episodic visual memory) among ALL survivors. In the right ventral cingulum, the fornix, and in the right uncinate fasciculus, RK correlated positively with scoring on Rey Auditory Verbal Learning Test (episodic verbal memory) among ALL survivors.

No significant correlations between DTI/DKI parameters and scoring on cognitive test were found among controls.

Paper V

When assessing cognitive interference processing, the reaction time was increased, and the accuracy performance was reduced during the interference tasks compared to the control tasks for the CP survivors, the two subgroups of CP survivors with and without hypothalamic involvement, respectively, and controls (Table 4). There were no significant differences in reaction time or accuracy performance in neither the interference nor the control tasks between the CP survivors, or the two subgroups, compared to the controls. The interference effect, regarded as the difference in reaction time and accuracy performance between the control and interference tasks was not significantly different between CP survivors and controls. Similar, no difference in the interference effect was seen between the CP subgroups and controls.

Table 4.
Reaction time and accuracy performance when assessing cognitive interference processing during the interference and control tasks in the multi-source interference task, as well as the interference effect, i.e., the difference in reaction time and accuracy performance between the interference and control tasks, for both adult childhood-onset craniopharyngioma survivors, the subgroup of craniophrayngioma subjects with and without hypothalamic involvement, respectively, and controls. Data are presented as median and quartile (first-third).

	Control task		Interference task		Interference effect	
	Reaction time (ms)	Accuracy performance (%)	Reaction time (ms)	Accuracy performance (%)	Difference in reaction time (ms)	Difference in accuracy performance (%)
CP patients ($n = 28$)	523.2 (485.8–576.6)	100.0 (99.5–100.0)	861.5 (786.3–926.1)	96.6 (93.8–98.4)	333.9 (287.3–367.1)[a]	3.1 (1.6–5.6)[a]
CP patients with HI ($n = 13$)	510.6 (490.3–582.1)	99.5 (99.0–100.0)	858.8 (789.5–919.0)	95.3 (93.5–97.7)	332.0 (283.6–353.4)[a]	4.2 (2.3–5.7)[a]
CP patients without HI ($n = 15$)	527.8 (475.4–575.5)	100.0 (100.0–100.0)	864.2 (780.0–948.6)	97.9 (94.8–99.0)	355.7 (293.7–388.7)[a]	2.1 (1.0–5.2)[a]
Controls ($n = 29$)	505.9 (453.3–541.9)	100.0 (99.5–100.0)	821.1 (770.4–891.5)	96.9 (94.8–97.9)	309.1 (276.4–361.0)[a]	2.6 (1.6–4.9)[a]

[a]Significant difference ($p < 0.05$) between interference and control tasks using the Wilcoxon signed-rank test.

CP = craniopharyngioma; HI = hypothalamic involvement.

The difference in fMRI activity required to perform the more cognitively demanding interference tasks compared to the control tasks, i.e. the interference effect, demonstrated fMRI activity in the CFP attention network in all the investigated groups (Figure 8). Comparisons between CP survivors and controls, the subgroups of CP survivors and controls showed no significant differences in fMRI activity between any of the groups.

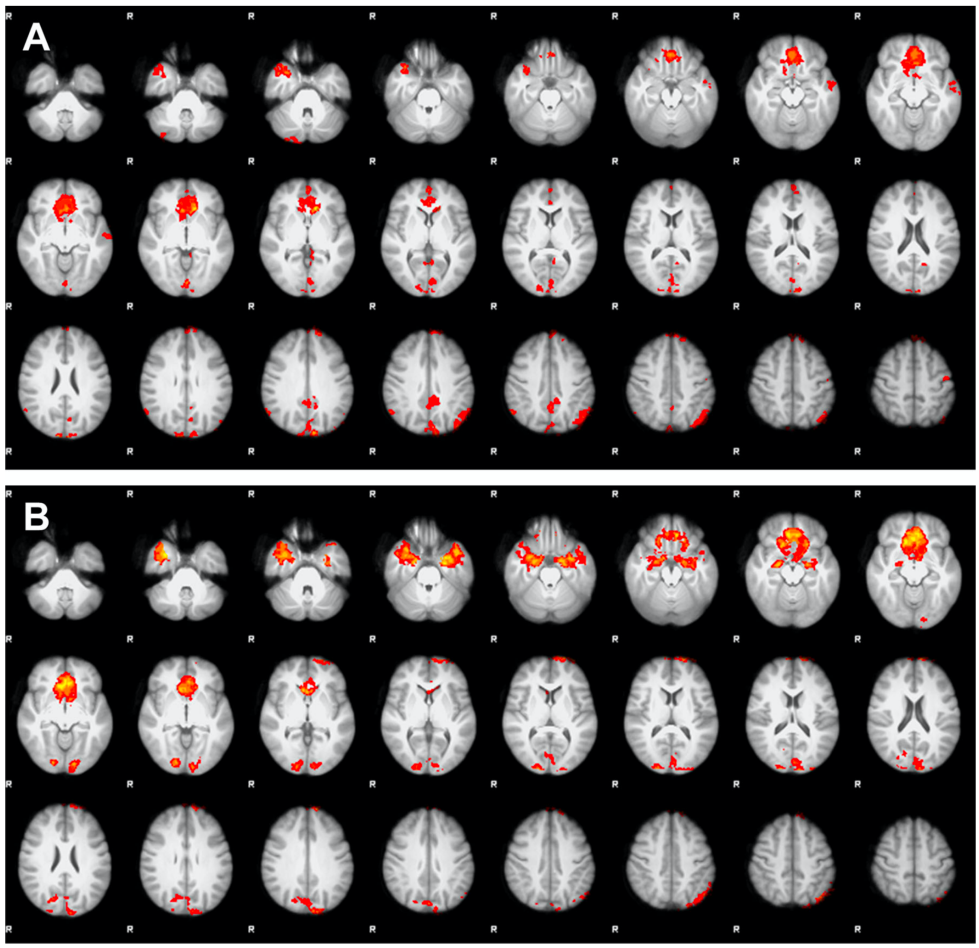

Figure 8.
Mean differences in whole-brain fMRI activity between the interference and control tasks in the multi-source interference task assessing cognitive interference processing, i.e. the difference in fMRI activity required to perform the additionally more cognitively demanding interference tasks, compared to the control tasks, revealed fMRI activity pattern in the cingulo-fronto-parietal attention network, but showed no significant differences between the adult childhood-onset craniopharyngioma (CP) survivors (A) and controls (B), the CP survivors with and without hypothalamic involvement (not shown here), respectively, and controls.

Paper VI

During cognitive interference processing, the interference effect, regarded as the difference in reaction time and accuracy performance between the control and interference tasks was increased and reduced, respectively, in ALL survivors compared to controls (Table 5). The ALL survivors exhibited increased reaction time during both interference and control tasks as compared to controls. The ALL

survivors also had reduced accuracy performance during interference tasks, but not during control tasks compared to controls. The reaction time was significantly increased during interference tasks compared to the control tasks for both ALL survivors and controls. The accuracy performance was significantly reduced during interference tasks as compared to the control tasks for both ALL survivors and controls. Additionally, all comparisons as detailed above were also performed for subgroups of males and females, respectively, with similar results.

Table 5.
Reaction time and accuracy performance during the interference and control tasks assessing cognitive interference processing with the multisource interference task, as well as the interference effect, i.e., the difference in reaction time and accuracy performance between the interference and control tasks, for both adult survivors of childhood-onset ALL and controls. Data are presented as median and quartile (first-third).

	Control task		Interference task		Interference effect	
	Reaction time (ms)	Accuracy performance (%)	Reaction time (ms)	Accuracy performance (%)	Difference in reaction time (ms)	Difference in accuracy performance (%)
ALL group ($n = 26$)	568.9 (520.0–630.7); $p = .002$	100.0 (99.5–100.0); $p = .9$	949.9 (897.5–1038.6); $p = .0002$	92.7 (84.9–95.8); $p = .0001$	371.9 (314.7–453.3); $p = .003$	6.7 (4.2–14.7); $p = .0001$
Control group ($n = 26$)	504.3 (454.0–538.8)	100.0 (99.5–100.0)	821.0 (769.8–884.7)	97.1 (95.6–97.9)	303.7 (275.0–376.7)	2.3 (1.6–4.3)

p-values are presented for comparison between the ALL survivors and controls using the Mann-Whitney *U* test.

ALL = acute lymphoblastic leukemia.

The difference in fMRI activity between interference and control tasks, i.e. the difference in neuronal activity required to perform the more cognitively demanding interference tasks as compared to the control tasks, revealed fMRI activity in the CFP attention network in both the ALL survivors and in the control group (Figure 9). Comparisons between ALL survivors and controls showed no differences in fMRI activity between the two groups. No significant differences between subgroups of males and females were present.

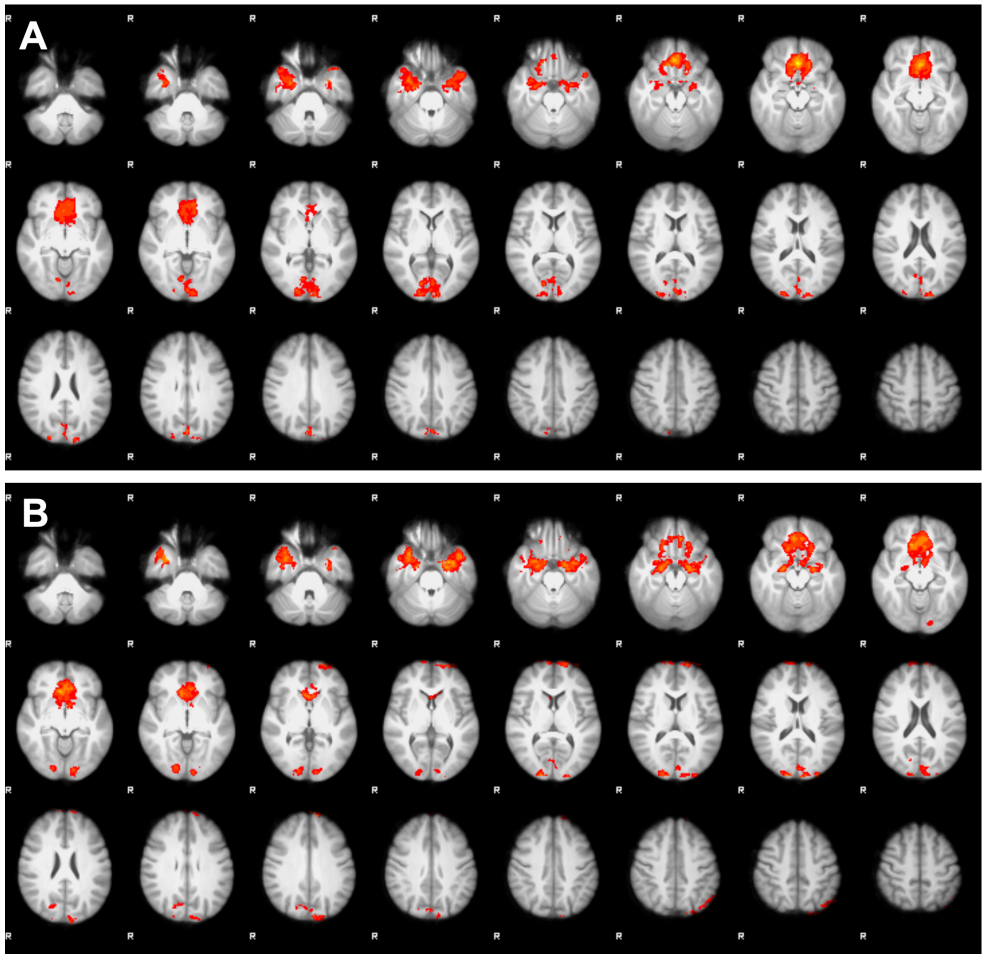

Figure 9.
Mean differences in whole-brain fMRI activity between the interference and control tasks in the multi-source interference task assessing cognitive interference processing, i.e. the difference in fMRI activity required to perform the additionally more cognitively demanding interference tasks compared to the control tasks, revealed fMRI activity pattern in the cingulo-fronto-parietal attention network, but showed no significant differences between the adult survivors of childhood-onset acute lymphoblastic leukemia (A) and controls (B).

Discussion

With this thesis, we set out to investigate structural and functional alterations in the brain and their association with cognition and metabolism in adult survivors of childhood-onset ALL and CP. To interpret the results correctly, we also investigated potential confounders of statistical dMRI analysis.

In paper I, we studied the effect of WMH on DTI parameters in several major WM tracts. We also assessed the effect of WMH on the results of a group comparison. We found that the effect of WMH on DTI parameters MD and FA were in general large. Moreover, in the group comparison, we found that adjusting the statistical analysis for WMH could improve the explanatory power of the analysis. Our interpretation is that the effect of WMH on DTI parameters is comparable to what has previously been reported for other conditions and that the results are of importance because they suggest that unequal WMH load in a group comparison could affect the outcome of the statistical analysis and thus lead to an over- or underestimation of disease-specific alterations.

In paper II, we studied microstructural alterations in the hypothalamus in adult survivors of childhood-onset ALL and CP without hypothalamic involvement using DTI. We found microstructural alterations in the hypothalamus in ALL survivors compared to controls but not in CP survivors without hypothalamic involvement. Further, these alterations were more pronounced in ALL survivors with BMI ≥ 25 compared to ALL survivors with BMI < 25. Our interpretation is that ALL survivors exhibit these microstructural alterations because of the CRT treatment they received compared to CP survivors without hypothalamic involvement. Further, it cannot be concluded whether the alterations in the hypothalamus in obese ALL survivors are the cause or the effect of obesity in these patients.

In paper III, we studied microstructural alterations in the cingulum, the fornix, the uncinate fasciculus, and in the hypothalamus in adult survivors of childhood-onset CP using DTI. We also assessed cognitive performance using cognitive tests and correlated the results to microstructural alterations in the abovementioned structures. We found microstructural alterations in the uncinate fasciculus in CP survivors compared to controls. We also found deficits in semantic memory, episodic verbal and visual memory, executive function, attention, and processing speed in CP survivors with hypothalamic involvement but not without hypothalamic involvement. Further, we found a correlation between microstructural alterations in

several of the investigated WM tracts and deficits in several of the investigated cognitive domains in CP survivors but not in controls. Our interpretation is that CP survivors present with deficits in several cognitive domains at least partially due to microstructural alterations in WM tracts adjacent to the surgically removed tumor. It cannot be concluded whether these microstructural alterations are due to the direct or indirect damage from the disease itself and/or its treatment.

In paper IV, we studied microstructural alterations in the cingulum, the fornix, and the uncinate fasciculus in adult survivors of childhood-onset ALL using DTI and DKI. We also assessed cognitive performance using cognitive tests and correlated the results to microstructural alterations in the abovementioned structures. We found microstructural alterations in several of the investigated WM tracts in ALL survivors compared to controls. We also found deficits in all of the investigated cognitive domains in ALL survivors compared to controls. Further, we found a correlation between microstructural alterations in several of the investigated WM tracts and deficits in several of the investigated cognitive domains in ALL survivors but not in controls. Our interpretation is that ALL survivors present with deficits in a wide variety of cognitive domains at least partially due to microstructural alterations in WM tracts partially connected to the hypothalamus, known to be sensitive to radiation. It cannot be concluded whether these microstructural alterations are due to direct or indirect damage from the treatment.

In paper V, we studied cognitive interference processing in terms of behavioral performance and fMRI activity in adult survivors of childhood-onset CP using the MSIT. We found a difference in both reaction time and accuracy performance as well as neuronal activity in the CFP attention network when performing the more cognitively demanding interference task compared to the control task in both CP survivors and controls. However, we did not find any differences in neither behavioral performance nor fMRI activity between the groups. Our interpretation is that CP survivors perform cognitive interference processing on the same level as controls without any compensatory neuronal activation.

In paper VI, we studied cognitive interference processing in terms of behavioral performance and fMRI activity in adult survivors of childhood-onset ALL using the MSIT. We found a difference in both reaction time and accuracy performance as well as neuronal activity in the CFP attention network when performing the more cognitively demanding interference task compared to the control task in both ALL survivors and controls. We also found reduced behavioral performance in ALL survivors compared to controls but no differences in fMRI activity. Our interpretation is that ALL survivors demonstrate deficits in cognitive interference processing compared to controls that cannot be explained with difference in neuronal activation as detected by fMRI.

Potential confounders in statistical analysis of dMRI

Compared to healthy WM that largely consists of densely packed axons, which restrict the diffusion of water molecules, pathological microstructural alterations in NAWM are thought to represent axonal loss and demyelination facilitating less restricted diffusion (Le Bihan, 2003). WMH, on the other hand, are thought to have a microstructure that consists of a varying degree of gliosis, and severe axonal loss and demyelination that also leads to less restricted diffusion (Fazekas et al., 1987; Jones et al., 1999; Gouw et al., 2011; Wardlaw et el., 2013). Early microstructural alterations in NAWM, detectable only with dMRI, are thought to be more disease-specific, whereas WMH, detectable with dMRI as well as T2-weigted MRI, are thought to represent a more unspecific end-stage of WM disease (Breteler et al., 1994; Ylikoski et al., 1995; Longstreth et al., 1996; de Leeuw et al., 2001; Kubicki et al., 2005; Sexton et al., 2011; Lebel et al., 2012; Santillo et al., 2013; Surova et al., 2015).

We found that the effect of WMH on DTI parameters MD and FA in cognitively healthy elderly was large and comparable to what has been previously reported for various conditions (Wang et al., 2004; Zhang et al., 2007; Gattellaro et al., 2009; Stenset et al., 2009; Zhuang et al., 2013; Rémy et al., 2015). Adjusting for potentially unequal levels of WMH between investigated groups might thus be necessary to disentangle effects of WMH from more disease-specific alterations in NAWM.

The largest effect sizes were observed in the SLF, which is partially located in regions where WMH are commonly observed (de Leeuw et al., 2001; Yoshita et al., 2006; Catani and de Schotten, 2008; Sexton et al., 2011). This suggests that there is a correlation between the effect of WMH on DTI parameters in a specific tract and its local WMH load. However, because the study in paper I was not designed to investigate this correlation, we can therefore neither confirm nor discard it.

When adjusting the analysis for WMH we observed that the explanatory power was improved for investigated WM tracts located in regions where WMH are common (e.g. the SLF) but not in regions were WMH are less common (e.g. the ventral cingulum) (de Leeuw et al., 2001; Yoshita et al., 2006; Catani and de Schotten, 2008). It is possible that these results can be extrapolated to other dMRI studies, in particularly in elderly subjects, since the prevalence of WMH is known to increase with age (Breteler et al., 1994; Ylikoski et al., 1995; Longstreth et al., 1996).

The conclusions from paper I made us consider WMH as a potential confounder in paper II–IV. Therefore, areas of the investigated WM tracts in paper II–IV were carefully inspected for WMH. WMH were present in some subjects, but not in areas where the investigated WM tracts were situated. Hence, in order not to reduce the statistical power of the statistical analyses, we decided not to adjust the statistical analyses for WMH in paper II-IV.

Structural alterations

Acute lymphoblastic leukemia

In paper II, we found that microstructural alterations in the hypothalamus in obese ALL survivors were more pronounced compared to non-obese. This is in concordance with a previous study also using DTI and reporting alterations in the hypothalamus in otherwise healthy obese subjects compared to non-obese (Alkan et al., 2007; Puig et al., 2015). In ALL survivors treated with CRT, BMI tends to increase with the follow-up time since diagnosis (Follin et al., 2010). It has also been shown that there is an association between reduced hypothalamic volume and increase in leptin/fat mass and fat mass in ALL survivors (Follin et al., 2016). Moreover, our finding may not be that surprising because obesity is known to be associated with hypothalamic inflammation in experimental models (Thaler et al., 2010). However, it is uncertain whether the structural alterations in the hypothalamus in ALL survivors are caused by obesity due to radiation-induced injury, or if they represent radiation-induced injury that has caused obesity. Patients with growth hormone deficiency or hypothyroidism have an increased metabolic risk (Maison et al., 2004; Feldt-Rasmussen and Klose, 2016). In contrast to other studies reporting an increased metabolic risk among ALL survivors treated with CRT, paper II is hitherto the only study where the ALL survivors were supplied with complete hormone substitution (Sklar et al., 2000; Link et al. 2004). Thus, it is not likely that the hypothalamic microstructural alterations were caused by hormone deficiency.

In paper IV, we found microstructural alterations using DTI in the uncinate fasciculus in ALL survivors compared to controls, and a correlation between these and deficits in episodic visual memory as tested using Rey Complex Figure Test. The uncinate fasciculus is the last of the major WM tracts to mature in the human brain, with complete myelination first seen in the fourth decade of life (Simmonds et al., 2014). It can be suspected that the neurotoxic effects of the treatment of ALL may affect the normal myelination process during childhood. Further, damage to the unmyelinated axons may result in deterioration of the tract leading to deficits in episodic memory later in life. The finding is also in line with a previous study showing that ALL survivors treated with CRT had reduced FA in the uncinate fasciculus (Schuitema et al., 2013).

The cingulum plays a critical role in structural connectivity of the brain for integrating information, including memory, with other parts of the brain, in particular the hippocampus. Reduced DKI parameters MK and RK were seen in both the dorsal and ventral cingulum, indicating altered microstructural integrity, which also correlated with reduced performance in episodic memory. Neurodegeneration of the cingulum is one of the earliest changes in development of

dementia (Metzler-Baddeley et al., 2012). The dorsal part of the cingulum is related to visual and spatial memory, whereas the ventral part is important for episodic memory (Wu et al., 2016). This is in line with our results, showing a correlation between MK and RK in the ventral cingulum and performance in episodic visual memory as tested using Rey Complex Figure Test, which tests how we remember specific events embedded in a spatial and temporal framework. Patients with Alzheimer's disease also exhibit microstructural alterations in the ventral cingulum, suggesting an increased risk of developing early-onset dementia (Parente et al., 2008).

DKI is theoretically more sensitive in detecting microstructural alterations in WM compared to DTI, especially in regions with complex fiber arrangement (Sotak, 2002). Previous studies on different conditions support this assumption (Hori et al., 2012; Gong et al., 2014). The DKI parameters MK and RK are, compared to the DTI parameter FA, a better description of the complexity of the organization of tissue microstructure, and are particularly useful when it comes to unravel microstructural integrity in major WM association fibers, such as the cingulum (Grinberg et al., 2017). The reduction of MK represents tissue degeneration that is likely to be associated with neuronal shrinkage and decreased axonal density (Jensen and Helpern, 2010; Wu and Cheung, 2010). Thus, using a combination of DTI and DKI will contribute to the existing knowledge in the field. Our results suggest larger effect sizes in DKI parameters compared with DTI, in particular when investigating the cingulum in ALL survivors, which is in line with previous reports. For example, larger effect sizes were seen in DKI parameters compared with DTI when studying maturation of WM (Grinberg et al., 2017).

CRT is known to have detrimental effects on brain development leading to cognitive impairment in ALL survivors (Campbell et al., 2007). However, we cannot exclude that the chemotherapy treatment directed to the CNS also may have a negative impact on the cognitive function in the survivors. In a previous long-term follow-up of ALL survivors treated with chemotherapy only, there were no deficiencies in general intellectual ability, impairment in processing speed, executive function and working memory (Kanellopoulos et al., 2016). However, other studies have reported cognitive impairment in ALL survivors treated with chemotherapy only (Halsey et al., 2011; Cheung and Krull, 2015).

The group of ALL survivors included in this thesis had been on complete hormone substitution, including GH, for median 10 years, which may improve cognitive function. Adults with childhood-onset GH deficiency due to other causes than ALL treatment have shown improvement in cognitive function with GH treatment (Oertel et al., 2004). However, in a previous study of ALL survivors, investigating cognitive performance before and after one year of GH therapy, an improvement in cognitive function could not be shown (Link et al., 2006) and results from the present study indicate that even long-term GH therapy cannot fully compensate for treatment related neuronal damage in this patient group.

Deficits in cognitive function in ALL survivors may lead to difficulties when it comes to higher education and employment (Haupt et al., 1994; Kingma et al., 2000). Among the subjects included in this thesis, only six of 38 ALL survivors reached university level. Further, 36% of the ALL survivors were unemployed, compared to 5% of the matched controls. Most of the survivors who were employed, had work tasks that required lower skills than the work tasks of the controls. Thus, the present results highlight a poor functional outcome regarding education level and working life in ALL survivors.

Craniopharyngioma

In paper III, we found that CP survivors had reduced FA and increased MD, suggesting microstructural alterations, in the right uncinate fasciculus, a tract known to be important for language and memory (Olson et al., 2015). In addition, reduced FA in this tract correlated with deficits in semantic memory. Importantly, no such correlation was found among the controls. It has previously been reported that CP survivors tend to have a lower level of education than controls (Fjalldal et al., 2013). This might partially be explained by degeneration of the uncinate fasciculus. It is also interesting that the uncinate fasciculus is usually one of the last of the major WM tracts to fully mature first in the early fourth decade of life (Lebel et al., 2012), which may make it particularly vulnerable to early treatment-induced tissue damage.

The ventral cingulum is highly connected to structures in the medial temporal lobe, and important for episodic memory (Wu et al., 2016). Interestingly, the strongest correlation we found was between microstructural alterations, indicated with increased MD, in the left ventral cingulum and deficits in episodic visual memory as tested using the Rey Complex Figure Test, explaining between 43–51% of the variation. This is in line with a prior study among patients with mild cognitive impairment and Alzheimer's disease, where early degeneration in the ventral cingulum was associated with a decline in episodic visual memory (Lin et al., 2014). We also found a correlation between altered microstructural integrity (increased MD) in the right dorsal cingulum and deficits in executive function. Deficits in executive function have previously been reported in CP survivors, but not previously been shown to be associated with neurodegeneration in a specific WM tract (Fjalldal et al., 2013; Özyurt et al., 2014b).

There are scarce data involving dMRI in the field of endocrinology (Resmini et al., 2012; Crespo et al., 2014; Özyurt et al., 2014b; Pires et al., 2015; Pires et al., 2017), and recent studies on cognitive function have instead focused on MRI volumetry, including cortical thickness (Resmini et al., 2012; Crespo et al., 2014; Özyurt et al., 2014b). The cingulate cortex, situated superficial to the cingulum, is involved in a variety of functions, including memory. A previous study on CP survivors found an association between grey matter volume of the posterior cingulate gyrus and

episodic memory, supporting the theory that hypothalamic involvement has an impact on GM volume outside of the area of the CP tumor (Özyurt et al., 2014b). Among patients with Cushing syndrome, widespread decreased WM integrity was seen using DTI and seemed to be independent of concomitant hypercortisolism and cardiovascular risk factors (Pires et al., 2015).

In CP survivors without hypothalamic involvement, no microstructural alterations as detected with DTI was found in the HT, which is in line with presumed better prognosis when it comes to cognitive and metabolic function compared to CP survivors with hypothalamic involvement (Fjalldal et al., 2013).

Functional alterations

Acute lymphoblastic leukemia

In paper VI, when assessing cognitive inteference processing with the MSIT, the ALL survivors needed longer time to complete the control tasks as well as the interference tasks compared to the controls. In addition, they performed less accurately during the more cognitively demanding interference tasks compared to the control group. The interference effect, i.e. the difference in reaction time was also longer, and the accuracy performance was reduced between the interference and control tasks in ALL survivors compared to the controls. Our results suggest that the effort needed to solve the more cognitively demanding interference tasks was greater in the ALL survivors than in the controls.

The interference effect was also studied regarding fMRI activity and revealed activation in the CFP attention network in both groups. Although there were differences in reaction time and accuracy performance between the investigated groups, the difference in fMRI activity that was needed to solve the more cognitively demanding interference tasks did not differ between the groups in neither the CFP attention network nor in any other areas of the brain. This suggests that the mechanism for the difference in cognitive performance between the ALL survivors and the control group was either too small to detect using this method or that it cannot be explained by alterations in functional networks in the brain.

The MSIT has previously been used to study alterations in behavioural performance and fMRI activity in different conditions, mostly within the field of psychiatry (Harrison et al., 2007; Yücel et al., 2007; Allen and Hooley, 2017; Capri et al., 2020), but also in patients with heart disease (Jung et al., 2018). The results have been highly varying regarding differences in fMRI activity (Harrison et al., 2007; Yücel et al., 2007) and most studies only reported behavioral performance (Allen and Hooley, 2017; Jung et al., 2018; Capri et al., 2020). In studies using fMRI,

decreased fMRI activity in the rostral anterior cingulate/medial prefrontal cortex and the precuneus/posterior cingulate cortex were seen in patients with schizophrenia (Harrison et al., 2007). In another study, increased fMRI activity was seen in the medial frontal cortex in patients with obsessive-compulsive disorder (Yücel et al., 2007). These somewhat ambiguous results might be due to different conditions affecting different parts of the brain. Further, the structures within the investigated area are responsible for different functions, so that decreased activity in one region could result in the same altered behavioral performance as increased activity in another region.

Results in neuroimaging studies on ALL survivors are highly variable, largely due to methodological variations, small sample-sizes, different treatment protocols, and different follow-up times (Hearps et al., 2017). Only five previous studies have used task-based fMRI to evaluate cognitive function in childhood-onset ALL (Robinson et al., 2010; Armstrong et al., 2013; Monje et al., 2013; Krull et al., 2016; Fellah et al., 2019). These previous studies have all used different fMRI tasks from the one used in paper VI, and therefore comparisons between findings can be challenging. However, our findings are in conjunction with one of the previous studies demonstrating similar findings in regard of similar behavioral performance in ALL survivors and controls in a study using the N-back task to assess working memory in eight teenage ALL survivors treated with intrathecal and intravenous chemotherapy (Robinson et al., 2010). Contradictory to our findings, the same study reported increased fMRI activity in the dACC and DLPFC. Even though the visual N-back task has been shown to partially activate the same regions as the MSIT (e.g. the dACC and the DLPFC) the task is different compared to what was used in the study in paper VI and hence the results are once again difficult to compare (Bush et al., 2003; Bush et al., 2006; Pesonen et al., 2007). Another study reported an increased fMRI activity in the hippocampus during an auditory cued-recall memory task in 85 adult ALL survivors treated with chemotherapy (intrathecal and intravenous) and radiotherapy (Armstrong et al., 2013). Increased fMRI activity in several areas throughout the brain including the claustrum during encoding of visual memories has also been reported in 10 adult ALL survivors treated with chemotherapy (intrathecal and intravenous) and radiotherapy (Monje et al. 2013). The same study also found that ALL survivors had differences in behavioral performance as compared to controls during the task, with lower recognition memory accuracy (Monje et al., 2013). Two studies performed the attention network test (Krull et al., 2016; Fellah et al., 2019). The first study found that higher plasma methotrexate during treatment was associated with higher fMRI activity in the frontal and anterior cingulate cortex, and in the caudate nuclei and the putamen in 142 teenage ALL survivors treated with intrathecal and intravenous chemotherapy (Krull et al., 2016). The other study found, somewhat contradictory, an association between decreased fMRI activity in the parietal and temporal lobes and the hippocampus during the attention network task and higher serum methotrexate

exposure in 165 teenage ALL survivors treated with intravenous methotrexate (Fellah et al., 2019).

Craniopharyngioma

In paper V, when assessing cognitive interference processing, we found that even though the interference effect in reaction time as well as accuracy performance was significant among both CP survivors and controls, there were no difference in neither reaction time nor accuracy performance between any of the investigated groups. Further, even though the MSIT activated the CFP attention network as expected, there were also no differences in fMRI activity between the groups. This suggests that the CP patients performed cognitive interference processing on a comparable level to the controls, without any compensatory fMRI activation.

Neuroimaging studies on childhood-onset CP are somewhat scarce. A few previous studies have demonstrated that WM integrity in the investigated areas correlated negatively to given radiation dose, reduced gray and WM volumes in the limbic areas, and have shown a negative correlation between long-term memory and gray matter in the posterior cingulate cortex (Uh et al., 2015; Özyurt et al., 2017).

Only two previous studies have used task-based fMRI to study cognitive impairment in childhood-onset CP survivors. These studies demonstrated lower fMRI activity during pre-meal test and higher fMRI activity during post-meal test as compared to controls (Roth et al., 2012) and differential recruitment of fronto-limbic brain regions during emotional face recognition (Özyurt et al., 2014b). Even though the hypothalamus is partially connected to the limbic system as well as partially to the CFP attention network, investigated in the present study, the investigated cognitive domains, chosen for evaluation, differs between the studies and therefore comparisons of the results to the results in paper V are difficult to interpret (Aggleton et al., 2011; Lemaire et al., 2011).

In comparison to previous studies on CP survivors that have demonstrated cognitive deficits, and functional and structural brain alterations, albeit using slightly different techniques and testing slightly different cognitive domains and neuroanatomical structures (Roth et al., 2012; Fjalldal et al., 2013; Özyurt et al., 2014b; Özyurt et al., 2015; Özyurt et al., 2017; Müller, 2019), the results in paper V may appear somewhat contradictory, as we did not find any functional alterations. However, not all previously investigated cognitive domains and/or neuroanatomical structures were affected. In this context, the results of the present study may not be that surprising.

Limitations

Paper I

When investigating WMH as a confounder in statistical analysis of DTI parameters, we identified some limitations. The exact etiology of WMH in the study population is not known, which means that WMH could in some subjects be an expression of another incipient disease for which dMRI could be sensitive. To minimize this potential confounding effect, we meticulously designed the inclusion and exclusion criteria. Further, WMH have different microscopic structure compared to NAWM, that may interfere with the tracking algorithm. Therefore, visual inspection of the generated tracts was performed, which gave no such suspicions. In addition, we also did not correct for multiple comparisons due to the explorative nature of the study in paper I. This means that we preferred the risk of accepting false positive differences over the risk of discarding true positive differences.

Paper II-VI

Because of the limited resolution of current dMRI technique, small structures like different nuclei in the hypothalamus cannot be investigated individually. Therefore, the microstructural alterations detected with dMRI in this thesis is an average estimation of the entire hypothalamus. This means that even though certain nuclei could have been of more interest compared to others, they cannot be studied in detail. It also means that even though large microstructural alterations may be present in one nucleus, this may not be detected if the volume of the nucleus is relatively small compared to the whole hypothalamus.

Further, cognitive function depends on complex neural networks, and it is not possible to relate a certain function to a single specific neural pathway. The study design does also not allow for any assumptions regarding causality nor the pathogenesis behind the altered microstructural integrity. For example, CRT was closely related to extensive re-operations and to hypothalamic involvement in CP survivors. Also, the necessary hormone replacement might to some degree have an impact on the present result.

The number of subjects was also limited, which may have led to an underpowered statistical analysis and thus an underestimation of the true differences when compared to controls. Only 8 CP survivors with hypothalamic involvement were included in the DTI analysis because of the difficulty to delineate the hypothalamus due to the hypothalamic lesion. Thus, the statistical analysis may have been underpowered leading to discarding of true differences.

Regarding the fMRI analysis, a potential selection bias might have been introduced when subjects who were unable to perform the task were excluded. Moreover, when it comes to the fMRI analysis, even though MSIT has been shown to reliably activate the CFP attention network, we chose an exploratory whole-brain fMRI

analysis approach instead of a ROI-based approach focusing on the area of the CFP attention network. This was to confirm that the MSIT activated the CFP attention network in these patient groups. We also wanted to study potential differences in fMRI activity in other areas of the brain that could indicate compensatory activation or deactivation due to neuronal damage. The disadvantage of a whole-brain analysis approach compared to a ROI-based analysis approach is however that the sensitivity for potential differences in activity in a specific area (e.g. the area of the CFP attention network) decreases.

Conclusions

In this thesis, we performed advanced neuroimaging in combination with neuropsychological, anthropometric, and biochemical assessment in four different cohorts and conclude that:

- WMH may act as a confounder in statistical analysis of dMRI parameters, but it depends on the specific study whether the analysis should be adjusted for this and in what way
- Adult survivors of childhood-onset ALL treated with CRT and chemotherapy demonstrated:
    - deficits in semantic memory, episodic verbal memory, episodic visual memory, working memory, executive function, attention, including sustained attention, and processing speed
    - microstructural alterations, as indicated using dMRI, in the hypothalamus that were more pronounced in obese compared to non-obese ALL survivors
    - microstructural alterations, as indicated using dMRI, in the dorsal and ventral cingulum, the fornix, and the uncinate fasciculus
    - a correlation between microstructural alterations, as indicated using dMRI, in some of the above-mentioned WM tracts and deficits in some of the abovementioned cognitive domains
    - deficits in cognitive interference processing but no related alteration in neuronal activity, as indicated using fMRI
- Adult survivors of childhood-onset CP treated with surgery and in some cases additional CRT demonstrated:
    - deficits in semantic memory, episodic verbal memory, episodic visual memory, executive function, attention, and processing speed if hypothalamic involvement was present
    - microstructural alterations, as indicated using dMRI, in the hypothalamus if hypothalamic involvement was present

- microstructural alterations, as indicated using dMRI, in the uncinate fasciculus
- a correlation between microstructural alterations, as indicated using dMRI, in the uncinate fasciculus and in the dorsal and ventral cingulum and deficits in some of the abovementioned cognitive domains
- no deficits in cognitive interference processing and no related alteration in neuronal activity, as indicated using fMRI

Clinical implications and future perspectives

Adult survivors of childhood-onset ALL and CP are both at risk of developing cognitive impairment and metabolic complications. Therefore, it is of importance to be able to optimize treatment regimens as well as follow-up care and support for these individuals. To achieve this, a better understanding of the underlaying pathophysiology of the disease as well as the side-effects of the treatment, including related late treatment complications, is crucial. The knowledge on the underlaying alterations in structural and functional networks in the brain in these patients are limited.

The findings presented in this thesis are an important further step towards increased knowledge when it comes to linking symptoms to structural and functional changes in the brain. This new knowledge may be useful when designing treatment protocols as well as for evaluation of late complications after treatment. In a more general perspective, the results may also improve the understanding of late treatment complications of other similar conditions.

From a methodological point of view, the conclusions on WMH as a confounder in statistical analysis of dMRI may be useful when designing and interpreting dMRI studies of other conditions. Further, the framework that was constructed to semi-automatically segment major WM tracts consistently and reliably have been extended during the work with this thesis and has so far been used in one other study not included in this thesis (Jalakas et al., 2019).

Further studies are needed to map what cognitive domains and metabolic functions are affected/unaffected in ALL and CP survivors and how these correlates to structural and functional alterations in the brain to better characterize the conditions. For example, a longitudinal study with baseline before treatment could be used to assess questions not answered in this thesis, such as if our findings are the result of direct or indirect damage to the investigated structures, and if our findings are the cause or effect of the cognitive and metabolic symptoms exhibited.

Populärvetenskaplig sammanfattning

Akut lymfatisk leukemi är en blodcancersjukdom som främst drabbar yngre barn. Behandlingen består av cellgiftsbehandling och i vissa fall även förebyggande strålbehandling mot olika områden av kroppen, som till exempel huvudet.

Kraniofaryngeom är en tumör som drabbar barn och medelålders vuxna. Tumören är godartad, men har ett aggressivt växtsätt och utgår från områden i hjärnan som kallas hypofysen och hypothalamus.

Barn som framgångsrikt behandlats för och överlevt någon av ovan nämnda sjukdomstillstånd uppvisar i vuxen ålder, i varierande grad, kognitiv funktionsnedsättning och problem med ämnesomsättningen. Den kognitiva funktionsnedsättningen innefattar bland annat brister i uppmärksamhet, minne samt uthållighet. Problemen med ämnesomsättningen innefattar främst en förhöjd risk att utveckla fetma. Man tror att dessa symtom beror på en kombination av sjukdomen i sig och dess respektive behandling. Mycket tyder på att skador i hypothalamus kan förklara en del av dessa symtom.

I denna avhandling använde vi oss av avancerad magnetkameraundersökning för att kartlägga strukturella och funktionella förändringar i hjärnan. Med strukturella förändringar menar vi förändringar i uppbyggnaden av olika strukturer i hjärnan och med funktionella förändringar hur kommunikationen mellan olika områden i hjärnan är förändrad. Vi använde oss även av neuropsykologiska tester för att kunna mäta olika kognitiva funktioner och vi analyserade förekomsten av olika näringsämnen och hormoner i blodet för att få en bild av hur ämnesomsättningen fungerar hos dessa individer. Denna information använde vi sedan för att försöka relatera kognitiv funktion och hur ämnesomsättningen är påverkad till de förändringar vi hittade i hjärnan.

I delarbete I undersökte vi förutsättningarna för hur man ska utföra och tolka resultaten när man tittar på strukturella förändringar i hjärnans vita substans. Vi kom fram till att man bör ta hänsyn till förekomstens av så kallade vitsubstansförändringar som ses vid småkärlssjukdom.

I delarbete II undersökte vi strukturella förändringar i hypothalamus. Våra resultat visar att man ser sådana förändringar hos vuxna som haft akut lymfatisk leukemi under barndomen och att dessa är mera uttalade hos de som också är överviktiga.

I delarbete III och IV undersökte vi kognitiv funktion hos vuxna som under barndomen haft akut lymfatisk leukemi eller kraniofaryngeom. Vi undersökte även strukturella förändringar i olika vitsubstansbanor, vilka alla är delvis kopplade till hypothalamus och är viktiga för olika kognitiva förmågor. Våra resultat visar att flera kognitiva funktioner är påverkade hos dessa patientgrupper och att det dessutom finns ett samband mellan denna påverkan och strukturella förändringar i de undersökta vitsubstansbanorna.

I delarbete V och VI undersökte vi hur försökspersonerna klarade av att hantera så kallad kognitiv interferens, vilket är förmågan att kunna fokusera på relevanta intryck och samtidigt undertrycka distraherande, irrelevanta sådana, och hur denna förmåga är relaterad till funktionella förändringar i hjärnan, alltså nervcellsaktivitet. Våra resultat visar att denna förmåga är nedsatt hos vuxna som under barndomen haft akut lymfatisk leukemi, men inte hos dem som haft kraniofaryngeom. Vi hittade däremot inga motsvarande funktionella förändringar i hjärnan, alltså förändringar i nervcellsaktivitet.

Sammanfattningsvis så har vi visat att vuxna som under barndomen drabbats av och behandlats framgångsrikt för akut lymfatisk leukemi eller kraniofaryngeom uppvisar kognitiva funktionsnedsättningar i varierande grad och att denna är relaterad till strukturella förändringar i olika delar av hjärnan. Våra resultat kan användas för att bättre kunna förstå dessa sjukdomstyper och därigenom även till att kunna förbättra behandlingsalternativen och den efterföljande understödjande behandlingen och rehabiliteringen.

Acknowledgements

First of all, I would like to start with thanking my main supervisor Cecilia Follin, my co-supervisors Eva Marie Erfurth, Markus Nilsson, and Pia Sundgren for being supportive, encouraging, and for believing that I someday would be able to actually complete this PhD project.

I would also like to thank Danielle van Westen for introducing me to neuroradiology and MRI research.

Also, thanks to Kasim Abul-Kasim for helping me when needed.

My co-authors, Isabella Björkman-Burtscher, Sigridur Fjalldal, Sanaz Gabery, Robin Hellerstedt, Aki Johanson, Björn Lampinen, Jimmy Lätt, Peter Mannfolk, Lennart Minthon, Johan Mårtensson, Åsa Petersén, Lars Rylander, Erik Stomrud, also deserve my gratitude for their many and important contributions. Without their expertise in different subjects, none of the papers in this thesis would have come into existence.

Some extra thanks to Oskar Hansson for letting me use the data from his cohorts.

Special thanks to Freddy Ståhlberg and the rest of the MR physics group for helping me with the challenging physics of MRI and for trying to make me think like a physicist instead of a physician. You all demonstrate a very high standard when it comes to research moral and have truly been a source of inspiration. Also, thanks to Titti Owman and Boel Hansson for taking care of me at the 7T facility.

I would also like to thank Peter Hochbergs for providing me with research time in the beginning of my project.

A special thanks to Markus Jacobson and Jan Blond for being understanding and for giving my plenty of valuable research time, which I truly needed to complete this PhD project.

I would also like to thank all my dear former residency colleagues at the Department of Medical Imaging and Physiology, Skåne University Hospital,

Malmö. You are a unique constellation of very kind, highly intelligent, and interesting people.

Special thanks to my friends for all the wisdom and craziness you've shared with me during my journey towards dissertation.

I would also like to thank the Bertenstam family for your kindness and support during some challenging years, not to mention all the intriguing scientific dinner discussions we've had.

My gratitude also to my family: My mother, Gun, my brother, Martin, and especially my father, Billy, for being supportive and encouraging.

Finally, my biggest gratitude goes to my partner and colleague, Malin Fredén Axelsson. Thank you for being there, for making me remember what really is important in life, and for proof-reading all my unexciting manuscripts!

References

Aggleton JP, Dumont JR, Warburton EC. Unraveling the contributions of the diencephalon to recognition memory: a review. Learn Mem. 2011;18(6):384-400.

Alexander AL, Lee JE, Lazar M, Field AS. Diffusion tensor imaging of the brain. Neurotherapeutics. 2007;4(3):316-329.

Alkan A, Sahin I, Keskin L, et al. Diffusion-weighted imaging features of brain in obesity. Magn Reson Imaging. 2008;26(4):446-450.

Allen KJ, Hooley JM. Negative mood and interference control in nonsuicidal self-injury. Compr Psychiatry. 2017;73:35-42.

Armstrong GT, Reddick WE, Petersen RC, et al. Evaluation of memory impairment in aging adult survivors of childhood acute lymphoblastic leukemia treated with cranial radiotherapy. J Natl Cancer Inst. 2013;105(12):899-907.

Arnold A. Effects of x-irradiation on the hypothalamus: a possible explanation for the therapeutic benefits following x-irradiation of the hypophysial region for pituitary dysfunction. J Clin Endocrinol Metab. 1954;14(8):859-868.

Basser PJ, Mattiello J, LeBihan D. MR diffusion tensor spectroscopy and imaging. Biophys J. 1994a;66(1):259-267.

Basser PJ, Mattiello J, LeBihan D. Estimation of the effective self-diffusion tensor from the NMR spin echo. J Magn Reson B. 1994b;103(3):247-254.

Basser PJ, Pajevic S, Pierpaoli C, Duda J, Aldroubi A. In vivo fiber tractography using DT-MRI data. Magn Reson Med. 2000;44(4):625-632.

Beckmann CF, Jenkinson M, Smith SM. General multilevel linear modeling for group analysis in FMRI. Neuroimage. 2003;20(2):1052-1063.

Behrens TE, Johansen-Berg H, Woolrich MW, et al. Non-invasive mapping of connections between human thalamus and cortex using diffusion imaging. Nat Neurosci. 2003;6(7):750-757.

Breteler MM, van Swieten JC, Bots ML, et al. Cerebral white matter lesions, vascular risk factors, and cognitive function in a population-based study: the Rotterdam Study. Neurology. 1994;44(7):1246-1252.

Bülow B, Attewell R, Hagmar L, Malmström P, Nordström CH, Erfurth EM. Postoperative prognosis in craniopharyngioma with respect to cardiovascular mortality, survival, and tumor recurrence. J Clin Endocrinol Metab. 1998;83(11):3897-3904.

Bunin GR, Surawicz TS, Witman PA, Preston-Martin S, Davis F, Bruner JM. The descriptive epidemiology of craniopharyngioma. J Neurosurg. 1998;89(4):547-551.

Bush G, Luu P, Posner MI. Cognitive and emotional influences in anterior cingulate cortex. Trends Cogn Sci. 2000;4(6):215-222.

Bush G, Shin LM, Holmes J, Rosen BR, Vogt BA. The Multi-Source Interference Task: validation study with fMRI in individual subjects. Mol Psychiatry. 2003;8(1):60-70.

Bush G, Shin LM. The Multi-Source Interference Task: an fMRI task that reliably activates the cingulo-frontal-parietal cognitive/attention network. Nat Protoc. 2006;1(1):308-313.

Campbell LK, Scaduto M, Sharp W, et al. A meta-analysis of the neurocognitive sequelae of treatment for childhood acute lymphocytic leukemia. Pediatr Blood Cancer. 2007;49(1):65-73.

Cannestra AF, Bookheimer SY, Pouratian N, et al. Temporal and topographical characterization of language cortices using intraoperative optical intrinsic signals. Neuroimage. 2000;12(1):41-54.

Capri T, Santoddi E, Fabio RA. Multi-Source Interference Task paradigm to enhance automatic and controlled processes in ADHD. Res Dev Disabil. 2020;97:103542.

Castillo EM, Simos PG, Davis RN, Breier J, Fitzgerald ME, Papanicolaou AC. Levels of word processing and incidental memory: dissociable mechanisms in the temporal lobe. Neuroreport. 2001;12(16):3561-3566.

Catani M, Thiebaut de Schotten M. A diffusion tensor imaging tractography atlas for virtual in vivo dissections. Cortex. 2008;44(8):1105-1132.

Chemaitilly W, Cohen LE, Mostoufi-Moab S, et al. Endocrine Late Effects in Childhood Cancer Survivors. J Clin Oncol. 2018;36(21):2153-2159.

Cheung YT, Krull KR. Neurocognitive outcomes in long-term survivors of childhood acute lymphoblastic leukemia treated on contemporary treatment protocols: A systematic review. Neurosci Biobehav Rev. 2015;53:108-120.

Crespo I, Esther GM, Santos A, et al. Impaired decision-making and selective cortical frontal thinning in Cushing's syndrome. Clin Endocrinol (Oxf). 2014;81(6):826-833.

Daianu M, Mendez MF, Baboyan VG, et al. An advanced white matter tract analysis in frontotemporal dementia and early-onset Alzheimer's disease. Brain Imaging Behav. 2016;10(4):1038-1053.

de Groot M, Ikram MA, Akoudad S, et al. Tract-specific white matter degeneration in aging: the Rotterdam Study. Alzheimers Dement. 2015;11(3):321-330.

de Leeuw FE, de Groot JC, Achten E, et al. Prevalence of cerebral white matter lesions in elderly people: a population based magnetic resonance imaging study. The Rotterdam Scan Study. J Neurol Neurosurg Psychiatry. 2001;70(1):9-14.

de Vile CJ, Grant DB, Hayward RD, Kendall BE, Neville BG, Stanhope R. Obesity in childhood craniopharyngioma: relation to post-operative hypothalamic damage shown by magnetic resonance imaging. J Clin Endocrinol Metab. 1996;81(7):2734-2737.

Douaud G, Jbabdi S, Behrens TE, et al. DTI measures in crossing-fibre areas: increased diffusion anisotropy reveals early white matter alteration in MCI and mild Alzheimer's disease. Neuroimage. 2011;55(3):880-890.

Douet V, Chang L. Fornix as an imaging marker for episodic memory deficits in healthy aging and in various neurological disorders. Front Aging Neurosci. 2015;6:343.

Edelstein K, D'agostino N, Bernstein LJ, et al. Long-term neurocognitive outcomes in young adult survivors of childhood acute lymphoblastic leukemia. J Pediatr Hematol Oncol. 2011;33(6):450-458.

Erfurth EM, Holmer H, Fjalldal SB. Mortality and morbidity in adult craniopharyngioma. Pituitary. 2013;16(1):46-55.

Fazekas F, Chawluk JB, Alavi A, Hurtig HI, Zimmerman RA. MR signal abnormalities at 1.5 T in Alzheimer's dementia and normal aging. AJR Am J Roentgenol. 1987;149(2):351-356.

Feldt-Rasmussen U, Klose M. Central hypothyroidism and its role for cardiovascular risk factors in hypopituitary patients. Endocrine. 2016;54(1):15-23.

Fellah S, Cheung YT, Scoggins MA, et al. Brain Activity Associated With Attention Deficits Following Chemotherapy for Childhood Acute Lymphoblastic Leukemia. J Natl Cancer Inst. 2019;111(2):201-209.

Fjalldal S, Holmer H, Rylander L, et al. Hypothalamic involvement predicts cognitive performance and psychosocial health in long-term survivors of childhood craniopharyngioma. J Clin Endocrinol Metab. 2013;98(8):3253-3262.

Fjalldal S, Follin C, Gabery S, et al. Detailed assessment of hypothalamic damage in craniopharyngioma patients with obesity. Int J Obes (Lond). 2019;43(3):533-544.

Follin C, Thilén U, Ahrén B, Erfurth EM. Improvement in cardiac systolic function and reduced prevalence of metabolic syndrome after two years of growth hormone (GH) treatment in GH-deficient adult survivors of childhood-onset acute lymphoblastic leukemia. J Clin Endocrinol Metab. 2006;91(5):1872-1875.

Follin C, Thilén U, Osterberg K, Björk J, Erfurth EM. Cardiovascular risk, cardiac function, physical activity, and quality of life with and without long-term growth hormone therapy in adult survivors of childhood acute lymphoblastic leukemia. J Clin Endocrinol Metab. 2010;95(8):3726-3735.

Follin C, Gabery S, Petersén Å, et al. Associations between Metabolic Risk Factors and the Hypothalamic Volume in Childhood Leukemia Survivors Treated with Cranial Radiotherapy. PLoS One. 2016;11(1):e0147575.

Folstein MF, Folstein SE, McHugh PR. "Mini-mental state". A practical method for grading the cognitive state of patients for the clinician. J Psychiatr Res. 1975;12(3):189-198.

Gabery S, Georgiou-Karistianis N, Lundh SH, et al. Volumetric analysis of the hypothalamus in Huntington Disease using 3T MRI: the IMAGE-HD Study. PLoS One. 2015;10(2):e0117593.

Gattellaro G, Minati L, Grisoli M, et al. White matter involvement in idiopathic Parkinson disease: a diffusion tensor imaging study. AJNR Am J Neuroradiol. 2009;30(6):1222-1226.

Gong G, Jiang T, Zhu C, et al. Asymmetry analysis of cingulum based on scale-invariant parameterization by diffusion tensor imaging. Hum Brain Mapp. 2005;24(2):92-98.

Gong NJ, Wong CS, Chan CC, Leung LM, Chu YC. Aging in deep gray matter and white matter revealed by diffusional kurtosis imaging. Neurobiol Aging. 2014;35(10):2203-2216.

Gouw AA, Seewann A, van der Flier WM, et al. Heterogeneity of small vessel disease: a systematic review of MRI and histopathology correlations. J Neurol Neurosurg Psychiatry. 2011;82(2):126-135.

Grinberg F, Maximov II, Farrher E, et al. Diffusion kurtosis metrics as biomarkers of microstructural development: A comparative study of a group of children and a group of adults. Neuroimage. 2017;144(Pt A):12-22.

Gustafsson G, Kreuger A, Dohlwitz A. Acute lymphoblastic leukemia in Swedish children 1973-1978. Acta Paediatr Scand. 1981;70(5):609-614.

Gustavsson AM, Stomrud E, Abul-Kasim K, et al. Cerebral Microbleeds and White Matter Hyperintensities in Cognitively Healthy Elderly: A Cross-Sectional Cohort Study Evaluating the Effect of Arterial Stiffness. Cerebrovasc Dis Extra. 2015;5(2):41-51.

Halsey C, Buck G, Richards S, Vargha-Khadem F, Hill F, Gibson B. The impact of therapy for childhood acute lymphoblastic leukaemia on intelligence quotients; results of the risk-stratified randomized central nervous system treatment trial MRC UKALL XI. J Hematol Oncol. 2011;4:42.

Harrison BJ, Yücel M, Pujol J, Pantelis C. Task-induced deactivation of midline cortical regions in schizophrenia assessed with fMRI. Schizophr Res. 2007;91(1-3):82-86.

Haupt R, Fears TR, Robison LL, et al. Educational attainment in long-term survivors of childhood acute lymphoblastic leukemia. JAMA. 1994;272(18):1427-1432.

Hearps S, Seal M, Anderson V, et al. The relationship between cognitive and neuroimaging outcomes in children treated for acute lymphoblastic leukemia with chemotherapy only: A systematic review. Pediatr Blood Cancer. 2017;64(2):225-233.

Holmer H, Ekman B, Björk J, et al. Hypothalamic involvement predicts cardiovascular risk in adults with childhood onset craniopharyngioma on long-term GH therapy. Eur J Endocrinol. 2009;161(5):671-679.

Holmer H, Pozarek G, Wirfält E, et al. Reduced energy expenditure and impaired feeding-related signals but not high energy intake reinforces hypothalamic obesity in adults with childhood onset craniopharyngioma. J Clin Endocrinol Metab. 2010;95(12):5395-5402.

Hori M, Fukunaga I, Masutani Y, et al. Visualizing non-Gaussian diffusion: clinical application of q-space imaging and diffusional kurtosis imaging of the brain and spine. Magn Reson Med Sci. 2012;11(4):221-233.

Howlader N, Noone AM, Krapcho M et al. SEER cancer statistics review, 1975–2017. National Cancer Institute. 2020.

Hua K, Zhang J, Wakana S, et al. Tract probability maps in stereotaxic spaces: analyses of white matter anatomy and tract-specific quantification. Neuroimage. 2008;39(1):336-347.

Insel N, Takehara-Nishiuchi K. The cortical structure of consolidated memory: a hypothesis on the role of the cingulate-entorhinal cortical connection. Neurobiol Learn Mem. 2013;106:343-350.

Jalakas M, Palmqvist S, Hall S, et al. A quick test of cognitive speed can predict development of dementia in Parkinson's disease. Sci Rep. 2019;9(1):15417.

Janelidze S, Zetterberg H, Mattsson N, et al. CSF Aβ42/Aβ40 and Aβ42/Aβ38 ratios: better diagnostic markers of Alzheimer disease. Ann Clin Transl Neurol. 2016;3(3):154-165.

Jardri R, Pins D, Bubrovszky M, et al. Self awareness and speech processing: an fMRI study. Neuroimage. 2007;35(4):1645-1653.

Jenkinson M, Smith S. A global optimisation method for robust affine registration of brain images. Med Image Anal. 2001;5(2):143-156.

Jenkinson M, Bannister P, Brady M, Smith S. Improved optimization for the robust and accurate linear registration and motion correction of brain images. Neuroimage. 2002;17(2):825-841.

Jenkinson M, Beckmann CF, Behrens TE, Woolrich MW, Smith SM. FSL. Neuroimage. 2012;62(2):782-790.

Jensen JH, Helpern JA. MRI quantification of non-Gaussian water diffusion by kurtosis analysis. NMR Biomed. 2010;23(7):698-710.

Jin J, Maren S. Prefrontal-Hippocampal Interactions in Memory and Emotion. Front Syst Neurosci. 2015;9:170.

Johansen-Berg H, Rushworth MF. Using diffusion imaging to study human connectional anatomy. Annu Rev Neurosci. 2009;32:75-94.

Jones DK, Lythgoe D, Horsfield MA, Simmons A, Williams SC, Markus HS. Characterization of white matter damage in ischemic leukoaraiosis with diffusion tensor MRI. Stroke. 1999;30(2):393-397.

Jung M, Jonides J, Berman MG, Northouse L, Koelling TM, Pressler SJ. Construct Validity of the Multi-Source Interference Task to Examine Attention in Heart Failure. Nurs Res. 2018;67(6):465-472.

Kanellopoulos A, Andersson S, Zeller B, et al. Neurocognitive Outcome in Very Long-Term Survivors of Childhood Acute Lymphoblastic Leukemia After Treatment with Chemotherapy Only. Pediatr Blood Cancer. 2016;63(1):133-138.

Kingma A, Rammeloo LA, van Der Does-van den Berg A, Rekers-Mombarg L, Postma A. Academic career after treatment for acute lymphoblastic leukaemia. Arch Dis Child. 2000;82(5):353-357.

Kirchhoff AC, Krull KR, Ness KK, et al. Physical, mental, and neurocognitive status and employment outcomes in the childhood cancer survivor study cohort. Cancer Epidemiol Biomarkers Prev. 2011;20(9):1838-1849.

Klein S, Staring M, Murphy K, Viergever MA, Pluim JP. elastix: a toolbox for intensity-based medical image registration. IEEE Trans Med Imaging. 2010;29(1):196-205.

Klingler J, Gloor P. The connections of the amygdala and of the anterior temporal cortex in the human brain. J Comp Neurol. 1960;115:333-369.

Koenig KA, Sakaie KE, Lowe MJ, et al. The relationship between cognitive function and high-resolution diffusion tensor MRI of the cingulum bundle in multiple sclerosis. Mult Scler. 2015;21(14):1794-1801.

Krull KR, Cheung YT, Liu W, et al. Chemotherapy Pharmacodynamics and Neuroimaging and Neurocognitive Outcomes in Long-Term Survivors of Childhood Acute Lymphoblastic Leukemia. J Clin Oncol. 2016;34(22):2644-2653.

Kubicki M, McCarley R, Westin CF, et al. A review of diffusion tensor imaging studies in schizophrenia. J Psychiatr Res. 2007;41(1-2):15-30.

Kunin-Batson A, Kadan-Lottick N, Zhu L, et al. Predictors of independent living status in adult survivors of childhood cancer: a report from the Childhood Cancer Survivor Study. Pediatr Blood Cancer. 2011;57(7):1197-1203.

Larkins RG, Martin FI. Hypopituitarism after extracranial irradiation: evidence for hypothalamic origin. Br Med J. 1973;1(5846):152-153.

Lätt J, Nilsson M, Wirestam R, et al. Regional values of diffusional kurtosis estimates in the healthy brain. J Magn Reson Imaging. 2013;37(3):610-618.

Le Bihan D, Mangin JF, Poupon C, et al. Diffusion tensor imaging: concepts and applications. J Magn Reson Imaging. 2001;13(4):534-546.

Le Bihan D. Looking into the functional architecture of the brain with diffusion MRI. Nat Rev Neurosci. 2003;4(6):469-480.

Lebel C, Gee M, Camicioli R, Wieler M, Martin W, Beaulieu C. Diffusion tensor imaging of white matter tract evolution over the lifespan. Neuroimage. 2012;60(1):340-352.

Lemaire JJ, Frew AJ, McArthur D, et al. White matter connectivity of human hypothalamus. Brain Res. 2011;1371:43-64.

Leritz EC, Shepel J, Williams VJ, et al. Associations between T1 white matter lesion volume and regional white matter microstructure in aging. Hum Brain Mapp. 2014;35(3):1085-1100.

Lin YC, Shih YC, Tseng WY, et al. Cingulum correlates of cognitive functions in patients with mild cognitive impairment and early Alzheimer's disease: a diffusion spectrum imaging study. Brain Topogr. 2014;27(3):393-402.

Link K, Moëll C, Garwicz S, et al. Growth hormone deficiency predicts cardiovascular risk in young adults treated for acute lymphoblastic leukemia in childhood. J Clin Endocrinol Metab. 2004;89(10):5003-5012.

Link K, Moëll C, Osterberg K, et al. Adult survivors of childhood acute lymphoblastic leukaemia with GH deficiency have normal self-rated quality of life but impaired neuropsychological performance 20 years after cranial irradiation. Clin Endocrinol (Oxf). 2006;65(5):617-625.

Littley MD, Shalet SM, Beardwell CG, Ahmed SR, Applegate G, Sutton ML. Hypopituitarism following external radiotherapy for pituitary tumours in adults. Q J Med. 1989;70(262):145-160.

Longstreth WT Jr, Manolio TA, Arnold A, et al. Clinical correlates of white matter findings on cranial magnetic resonance imaging of 3301 elderly people. The Cardiovascular Health Study. Stroke. 1996;27(8):1274-1282.

Lustig RH, Post SR, Srivannaboon K, et al. Risk factors for the development of obesity in children surviving brain tumors. J Clin Endocrinol Metab. 2003;88(2):611-616.

Maillard P, Fletcher E, Harvey D, et al. White matter hyperintensity penumbra. Stroke. 2011;42(7):1917-1922.

Maillard P, Fletcher E, Lockhart SN, et al. White matter hyperintensities and their penumbra lie along a continuum of injury in the aging brain. Stroke. 2014;45(6):1721-1726.

Maison P, Griffin S, Nicoue-Beglah M, et al. Impact of growth hormone (GH) treatment on cardiovascular risk factors in GH-deficient adults: a Metaanalysis of Blinded, Randomized, Placebo-Controlled Trials. J Clin Endocrinol Metab. 2004;89(5):2192-2199.

Manjer J, Carlsson S, Elmståhl S, et al. The Malmö Diet and Cancer Study: representativity, cancer incidence and mortality in participants and non-participants. Eur J Cancer Prev. 2001;10(6):489-499.

Martín-Loeches M, Casado P, Hernández-Tamames JA, Alvarez-Linera J. Brain activation in discourse comprehension: a 3t fMRI study. Neuroimage. 2008;41(2):614-622.

Menon V. Large-scale brain networks and psychopathology: a unifying triple network model. Trends Cogn Sci. 2011;15(10):483-506.

Menon V, Uddin LQ. Saliency, switching, attention and control: a network model of insula function. Brain Struct Funct. 2010;214(5-6):655-667.

Menzler K, Belke M, Unger MM, et al. DTI reveals hypothalamic and brainstem white matter lesions in patients with idiopathic narcolepsy. Sleep Med. 2012;13(6):736-742.

Merchant TE, Kiehna EN, Sanford RA, et al. Craniopharyngioma: the St. Jude Children's Research Hospital experience 1984-2001. Int J Radiat Oncol Biol Phys. 2002;53(3):533-542.

Metzler-Baddeley C, Jones DK, Steventon J, Westacott L, Aggleton JP, O'Sullivan MJ. Cingulum microstructure predicts cognitive control in older age and mild cognitive impairment. J Neurosci. 2012;32(49):17612-17619.

Mody R, Li S, Dover DC, et al. Twenty-five-year follow-up among survivors of childhood acute lymphoblastic leukemia: a report from the Childhood Cancer Survivor Study. Blood. 2008;111(12):5515-5523.

Monje M, Thomason ME, Rigolo L, et al. Functional and structural differences in the hippocampus associated with memory deficits in adult survivors of acute lymphoblastic leukemia. Pediatr Blood Cancer. 2013;60(2):293-300.

Mori S, Barker PB. Diffusion magnetic resonance imaging: its principle and applications. Anat Rec. 1999;257(3):102-109.

Mori S, Wakana S, Nagae-Poetscher LM, van Zijl PCM. MRI atlas of human white matter. Elsevier, Amsterdam, The Netherlands 2005.

Müller HL. Consequences of craniopharyngioma surgery in children. J Clin Endocrinol Metab. 2011;96(7):1981-1991.

Müller HL. Childhood craniopharyngioma. Pituitary. 2013;16(1):56-67.

Müller HL. Risk-adapted, long-term management in childhood-onset craniopharyngioma. Pituitary. 2017;20(2):267-281.

Müller HL. MANAGEMENT OF ENDOCRINE DISEASE: Childhood-onset craniopharyngioma: state of the art of care in 2018. Eur J Endocrinol. 2019;180(4):R159-R174.

Müller HL, Emser A, Faldum A, et al. Longitudinal study on growth and body mass index before and after diagnosis of childhood craniopharyngioma. J Clin Endocrinol Metab. 2004;89(7):3298-3305.

Müller HL, Gebhardt U, Teske C, et al. Post-operative hypothalamic lesions and obesity in childhood craniopharyngioma: results of the multinational prospective trial KRANIOPHARYNGEOM 2000 after 3-year follow-up. Eur J Endocrinol. 2011;165(1):17-24.

Newton JM, Ward NS, Parker GJ, et al. Non-invasive mapping of corticofugal fibres from multiple motor areas--relevance to stroke recovery. Brain. 2006;129(Pt 7):1844-1858.

Nørhøj Jespersen S. White matter biomarkers from diffusion MRI. J Magn Reson. 2018;291:127-140.

Nucifora PG, Wu X, Melhem ER, Gur RE, Gur RC, Verma R. Automated diffusion tensor tractography: implementation and comparison to user-driven tractography. Acad Radiol. 2012;19(5):622-629.

Ochs J, Mulhern R, Fairclough D, et al. Comparison of neuropsychologic functioning and clinical indicators of neurotoxicity in long-term survivors of childhood leukemia given cranial radiation or parenteral methotrexate: a prospective study. J Clin Oncol. 1991;9(1):145-151.

Oertel H, Schneider HJ, Stalla GK, Holsboer F, Zihl J. The effect of growth hormone substitution on cognitive performance in adult patients with hypopituitarism. Psychoneuroendocrinology. 2004;29(7):839-850.

Ogawa S, Lee TM, Kay AR, Tank DW. Brain magnetic resonance imaging with contrast dependent on blood oxygenation. Proc Natl Acad Sci U S A. 1990;87(24):9868-9872.

Ogawa S, Tank DW, Menon R, et al. Intrinsic signal changes accompanying sensory stimulation: functional brain mapping with magnetic resonance imaging. Proc Natl Acad Sci U S A. 1992;89(13):5951-5955.

Olson IR, Von Der Heide RJ, Alm KH, Vyas G. Development of the uncinate fasciculus: Implications for theory and developmental disorders. Dev Cogn Neurosci. 2015;14:50-61.

Olsson DS, Andersson E, Bryngelsson IL, Nilsson AG, Johannsson G. Excess mortality and morbidity in patients with craniopharyngioma, especially in patients with childhood onset: a population-based study in Sweden. J Clin Endocrinol Metab. 2015;100(2):467-474.

Özyurt J, Thiel CM, Lorenzen A, et al. Neuropsychological outcome in patients with childhood craniopharyngioma and hypothalamic involvement. J Pediatr. 2014a;164(4):876-881.e4.

Özyurt J, Lorenzen A, Gebhardt U, Warmuth-Metz M, Müller HL, Thiel CM. Remote effects of hypothalamic lesions in the prefrontal cortex of craniopharygioma patients. Neurobiol Learn Mem. 2014b;111:71-80.

Özyurt J, Müller HL, Thiel CM. A systematic review of cognitive performance in patients with childhood craniopharyngioma. J Neurooncol. 2015;125(1):9-21.

Özyurt J, Müller HL, Warmuth-Metz M, Thiel CM. Hypothalamic tumors impact gray and white matter volumes in fronto-limbic brain areas. Cortex. 2017;89:98-110.

Parente DB, Gasparetto EL, da Cruz LC Jr, et al. Potential role of diffusion tensor MRI in the differential diagnosis of mild cognitive impairment and Alzheimer's disease. AJR Am J Roentgenol. 2008;190(5):1369-1374.

Park HJ, Westin CF, Kubicki M, et al. White matter hemisphere asymmetries in healthy subjects and in schizophrenia: a diffusion tensor MRI study. Neuroimage. 2004;23(1):213-223.

Pelletier A, Periot O, Dilharreguy B, et al. Age-Related Modifications of Diffusion Tensor Imaging Parameters and White Matter Hyperintensities as Inter-Dependent Processes. Front Aging Neurosci. 2016;7:255.

Pereira AM, Schmid EM, Schutte PJ, et al. High prevalence of long-term cardiovascular, neurological and psychosocial morbidity after treatment for craniopharyngioma. Clin Endocrinol (Oxf). 2005;62(2):197-204.

Pesonen M, Hämäläinen H, Krause CM. Brain oscillatory 4-30 Hz responses during a visual n-back memory task with varying memory load. Brain Res. 2007;1138:171-177.

Pierpaoli C, Jezzard P, Basser PJ, Barnett A, Di Chiro G. Diffusion tensor MR imaging of the human brain. Radiology. 1996;201(3):637-648.

Pires P, Santos A, Vives-Gilabert Y, et al. White matter alterations in the brains of patients with active, remitted, and cured cushing syndrome: a DTI study. AJNR Am J Neuroradiol. 2015;36(6):1043-1048.

Pires P, Santos A, Vives-Gilabert Y, et al. White matter involvement on DTI-MRI in Cushing's syndrome relates to mood disturbances and processing speed: a case-control study. Pituitary. 2017;20(3):340-348.

Plasschaert SL, Kamps WA, Vellenga E, de Vries EG, de Bont ES. Prognosis in childhood and adult acute lymphoblastic leukaemia: a question of maturation?. Cancer Treat Rev. 2004;30(1):37-51.

Potter GM, Doubal FN, Jackson CA, et al. Counting cavitating lacunes underestimates the burden of lacunar infarction. Stroke. 2010;41(2):267-272.

Puig J, Blasco G, Daunis-I-Estadella J, et al. Hypothalamic damage is associated with inflammatory markers and worse cognitive performance in obese subjects. J Clin Endocrinol Metab. 2015;100(2):E276-E281.

Raichle ME. The brain's default mode network. Annu Rev Neurosci. 2015;38:433-447.

Rahmathulla G, Marko NF, Weil RJ. Cerebral radiation necrosis: a review of the pathobiology, diagnosis and management considerations. J Clin Neurosci. 2013;20(4):485-502.

Rémy F, Vayssière N, Saint-Aubert L, Barbeau E, Pariente J. White matter disruption at the prodromal stage of Alzheimer's disease: relationships with hippocampal atrophy and episodic memory performance. Neuroimage Clin. 2015;7:482-492. Published 2015 Jan 27.

Resmini E, Santos A, Gómez-Anson B, et al. Verbal and visual memory performance and hippocampal volumes, measured by 3-Tesla magnetic resonance imaging, in patients with Cushing's syndrome. J Clin Endocrinol Metab. 2012;97(2):663-671.

Robinson KE, Livesay KL, Campbell LK, et al. Working memory in survivors of childhood acute lymphocytic leukemia: functional neuroimaging analyses. Pediatr Blood Cancer. 2010;54(4):585-590.

Roth CL, Aylward E, Liang O, Kleinhans NM, Pauley G, Schur EA. Functional neuroimaging in craniopharyngioma: a useful tool to better understand hypothalamic obesity?. Obes Facts. 2012;5(2):243-253.

Sabsevitz DS, Medler DA, Seidenberg M, Binder JR. Modulation of the semantic system by word imageability. Neuroimage. 2005;27(1):188-200.

Santillo AF, Mårtensson J, Lindberg O, et al. Diffusion tensor tractography versus volumetric imaging in the diagnosis of behavioral variant frontotemporal dementia. PLoS One. 2013;8(7):e66932. Published 2013 Jul 18.

Sathiavageeswaran M, Burman P, Lawrence D, et al. Effects of GH on cognitive function in elderly patients with adult-onset GH deficiency: a placebo-controlled 12-month study. Eur J Endocrinol. 2007;156(4):439-447.

Schmidt R, Schmidt H, Haybaeck J, et al. Heterogeneity in age-related white matter changes. Acta Neuropathol. 2011;122(2):171-185.

Schneeberger M, Gomis R, Claret M. Hypothalamic and brainstem neuronal circuits controlling homeostatic energy balance. J Endocrinol. 2014;220(2):T25-T46.

Schubert T, Trippel M, Tacke U, et al. Neurosurgical treatment strategies in childhood craniopharyngiomas: is less more?. Childs Nerv Syst. 2009;25(11):1419-1427.

Schuitema I, Deprez S, Van Hecke W, et al. Accelerated aging, decreased white matter integrity, and associated neuropsychological dysfunction 25 years after pediatric lymphoid malignancies. J Clin Oncol. 2013;31(27):3378-3388.

Schuitema I, de Sonneville L, Kaspers G, et al. Executive Dysfunction 25 Years after Treatment with Cranial Radiotherapy for Pediatric Lymphoid Malignancies. J Int Neuropsychol Soc. 2015;21(9):657-669.

Sexton CE, Kalu UG, Filippini N, Mackay CE, Ebmeier KP. A meta-analysis of diffusion tensor imaging in mild cognitive impairment and Alzheimer's disease. Neurobiol Aging. 2011;32(12):.

Simmonds DJ, Hallquist MN, Asato M, Luna B. Developmental stages and sex differences of white matter and behavioral development through adolescence: a longitudinal diffusion tensor imaging (DTI) study. Neuroimage. 2014;92:356-368.

Sklar CA, Mertens AC, Walter A, et al. Changes in body mass index and prevalence of overweight in survivors of childhood acute lymphoblastic leukemia: role of cranial irradiation. Med Pediatr Oncol. 2000;35(2):91-95.

Smith SM. Fast robust automated brain extraction. Hum Brain Mapp. 2002;17(3):143-155.

Sotak CH. The role of diffusion tensor imaging in the evaluation of ischemic brain injury - a review. NMR Biomed. 2002;15(7-8):561-569.

Stenset V, Bjørnerud A, Fjell AM, et al. Cingulum fiber diffusivity and CSF T-tau in patients with subjective and mild cognitive impairment. Neurobiol Aging. 2011;32(4):581-589.

Surova Y, Nilsson M, Lätt J, et al. Disease-specific structural changes in thalamus and dentatorubrothalamic tract in progressive supranuclear palsy. Neuroradiology. 2015;57(11):1079-1091.

Thaler JP, Choi SJ, Schwartz MW, Wisse BE. Hypothalamic inflammation and energy homeostasis: resolving the paradox. Front Neuroendocrinol. 2010;31(1):79-84.

Tomlinson JW, Holden N, Hills RK, et al. Association between premature mortality and hypopituitarism. West Midlands Prospective Hypopituitary Study Group. Lancet. 2001;357(9254):425-431.

Tournier JD, Calamante F, Connelly A. Robust determination of the fibre orientation distribution in diffusion MRI: non-negativity constrained super-resolved spherical deconvolution. Neuroimage. 2007;35(4):1459-1472.

Uddin LQ, Yeo BTT, Spreng RN. Towards a Universal Taxonomy of Macro-scale Functional Human Brain Networks. Brain Topogr. 2019;32(6):926-942.

Uh J, Merchant TE, Li Y, et al. Effects of Surgery and Proton Therapy on Cerebral White Matter of Craniopharyngioma Patients. Int J Radiat Oncol Biol Phys. 2015;93(1):64-71.

Vernooij MW, de Groot M, van der Lugt A, et al. White matter atrophy and lesion formation explain the loss of structural integrity of white matter in aging. Neuroimage. 2008;43(3):470-477.

Wakana S, Caprihan A, Panzenboeck MM, et al. Reproducibility of quantitative tractography methods applied to cerebral white matter. Neuroimage. 2007;36(3):630-644.

Wang F, Sun Z, Cui L, et al. Anterior cingulum abnormalities in male patients with schizophrenia determined through diffusion tensor imaging. Am J Psychiatry. 2004;161(3):573-575.

Wardlaw JM, Smith EE, Biessels GJ, et al. Neuroimaging standards for research into small vessel disease and its contribution to ageing and neurodegeneration. Lancet Neurol. 2013;12(8):822-838.

Woolrich M. Robust group analysis using outlier inference. Neuroimage. 2008;41(2):286-301.

Woolrich MW, Ripley BD, Brady M, Smith SM. Temporal autocorrelation in univariate linear modeling of FMRI data. Neuroimage. 2001;14(6):1370-1386.

Woolrich MW, Behrens TE, Beckmann CF, Jenkinson M, Smith SM. Multilevel linear modelling for FMRI group analysis using Bayesian inference. Neuroimage. 2004;21(4):1732-1747.

Wu EX, Cheung MM. MR diffusion kurtosis imaging for neural tissue characterization. NMR Biomed. 2010;23(7):836-848.

Wu Y, Sun D, Wang Y, Wang Y, Ou S. Segmentation of the Cingulum Bundle in the Human Brain: A New Perspective Based on DSI Tractography and Fiber Dissection Study. Front Neuroanat. 2016;10:84.

Ylikoski A, Erkinjuntti T, Raininko R, Sarna S, Sulkava R, Tilvis R. White matter hyperintensities on MRI in the neurologically nondiseased elderly. Analysis of

cohorts of consecutive subjects aged 55 to 85 years living at home. Stroke. 1995;26(7):1171-1177.

Yoshita M, Fletcher E, Harvey D, et al. Extent and distribution of white matter hyperintensities in normal aging, MCI, and AD. Neurology. 2006;67(12):2192-2198.

Yücel M, Harrison BJ, Wood SJ, et al. Functional and biochemical alterations of the medial frontal cortex in obsessive-compulsive disorder. Arch Gen Psychiatry. 2007;64(8):946-955.

Zhang Y, Schuff N, Jahng GH, et al. Diffusion tensor imaging of cingulum fibers in mild cognitive impairment and Alzheimer disease. Neurology. 2007;68(1):13-19.

Zhuang L, Sachdev PS, Trollor JN, et al. Microstructural white matter changes, not hippocampal atrophy, detect early amnestic mild cognitive impairment. PLoS One. 2013;8(3):e58887.

Daniel Svärd completed his medical degree at Lund University in 2013 and became a PhD student the same year. He did his internship as a physician at Skåne University Hospital in Lund between 2013-2015, and his residency in radiology at Skåne University Hospital in Lund and Malmö between 2015-2021. In 2021, he completed his PhD degree. This publication is his doctoral thesis.

Printed by Media-Tryck, Lund 2021 NORDIC SWAN ECOLABEL 3041 0903

LUND UNIVERSITY

FACULTY OF MEDICINE

Department of Clinical Sciences, Lund

Lund University, Faculty of Medicine
Doctoral Dissertation Series 2021:95
ISBN 978-91-8021-102-4
ISSN 1652-8220